Error propagation in hydrodynamics of lowland rivers due to uncertainty in vegetation roughness parameterization

Menno Straatsma, Dinand Alkema

ITC-FC2015 report:2009.06.05

ITC International Institute for Geo-Information Science and Earth Observation

Error propagation in hydrodynamics of lowland rivers due to uncertainty in vegetation roughness parameterization

ITC-FC2015 report:2009.06.05
Corresponding author: Menno Straatsma
Email: Straatsma@itc.nl
Status: final

Table of contents

Abstract

Accurate water level prediction for the design discharge of large rivers is of main importance for the flood safety of large embanked areas in The Netherlands. Within a larger framework of uncertainty assessment, this report focusses on the effect of uncertainty in roughness parameterization in a 2D hydrodynamic model. Two key elements are considered in this roughness parameterization. Firstly the manually classified ecotope map that provides base data for roughness classes, and secondly the lookup table that translates roughness classes to vegetation structural characteristics. The aim is to quantify the sensitivity of the model to these error sources, assessed by:

1. the discharge distribution at the bifurcation points within the river Rhine the design discharge of 16 000 m^3/s
2. the peak water levels at the design discharge.

To assess the effect of the first error source, new realisations of ecotope maps were made based on the current ecotope map and an error matrix of the classification. Using these realisations of the ecotope maps, twelve succesfull model runs were carried out of the Rhine distributaries at design discharge. The classification error leads to a standard deviation of the water levels per river kilometer of 0.08, 0.05 and 0.10 m for Upper Rhine- Waal, Pannerdensch Kanaal-Nederrijn-Lek and the IJssel river respectively. The maximum range in water levels is 0.40, 0.40 and 0.57 m for these river sections respectively. Largest effects are found in the IJssel river and the Pannerdensch Kanaal. These results show the sensitivity to roughness parameterisation. It is **not the absolute uncertainty** in the peak flood levels of the design discharge as calibration will limit the absolute uncertainty to a large extent. Therefore the results should also not be interpreted as the required increase in the height of the embankments.

For the second error source, the accuracy of the values in the lookup table, a compilation was made of 445 field measurements of vegetation structure was carried out. For each of the vegetation types, the minimum, 25-percentile, median, 75-percentile and maximum for vegetation height and density were computed. These five values were subsequently put in the lookup table that was used for the hydrodynamic model. The interquartile range in vegetation height and density in the lookup table led to a difference in water levels of 0.20, 0.20, and 0.36 m for Upper Rhine- Waal, Pannerdensch Kanaal-Nederrijn-Lek and the IJssel river respectively. These uncertainties are based on a maximum variation in vegetation structure to get an impression of the range in water levels.

The discharge distribution at the Pannerdensche Kop bifurcation point is 165 m^3/s for both error sources, classification and lookup table. The discharge distribution at the IJsselkop is more sensitive for classification errors (range of 160 m^3/s) than for errors in the lookup table (interquartile range of 70 m^3/s). The range in classification error and interquartile range in lookup table error. Priority should be given to increasing the classification accuracy as this generates the largest error for water levels as well as discharge distribution.

The quantification of the uncertainty in water levels and discharge distribution will help to make decisions more realistically as the error bands are substantiated. These are still relative differences and not absolute accuracies of the model output after calibration, but it may serve as a first step. Moreover, the error bands may serve as an incentive to quantify the desired accuracy in the vegetation structural characteristics. This means that an upper limit can be put on the variation in water levels that is accepted from errors in the roughness parameterization.

1. Introduction

Accurate water level prediction for the design discharge of large rivers is of main importance for the flood safety of large embanked areas in The Netherlands. In 2015 the design discharge for the river Rhine and its distributaries is set to 16000 m^3/s, corresponding to an annual probability of 1/1250. The distribution of water over the Rhine branches and the resulting water levels depends on the bathymetry of the river and the hydrodynamic roughness of the main channel and the floodplain. The modeling of the water levels is bound with uncertainty due to the complexity of the input and the various schematizations of the interaction between the water and the river bed.

Walker et al. (2003) defined uncertainty as “any departure from the unachievable ideal of complete determinism.” They further distinguished three aspects of uncertainty related to location, level, and nature of the uncertainty. The location uncertainty relates to where the uncertainty manifests in the model complex and depends on the context, model uncertainty, input, parameter uncertainty and outcome uncertainty. The level of uncertainty relates to the point on a scale ranging from statistical uncertainty, scenario uncertainty, to recognized ignorance and down to total ignorance. The third component nature of uncertainty comprises the distinction between inherent, or epistemic uncertainty and variability uncertainty. These three component can be mapped onto a matrix that describes all components of uncertainty for a specific problem.

Van der Klis et el. (2006) filled such an uncertainty matrix following Walker et al. (2003) with respect to the uncertainties in the hydraulic boundary conditions of the Rhine branches. This included eighteen aspects that were mapped onto the matrix. Aspects included seasonal variation in vegetation, morphodynamics, management, climate change, model structure, grid resolution, shape of the discharge curve, roughness equations, formulation for energy loss over barriers, boundary conditions, and lateral influxes of water. Following a qualitative approach, they concluded that the uncertainty related to the roughness parameterization of the main channel and the floodplain has a fairly large effect on the modeled water levels. A quantitative approach was followed to determine the effect of morphological changes in the main channel by Van der Klis (2003) and Van Vuren (2005). The effects were most relevant for low water navigability.

Within this multitude of sources of uncertainty, we focus on the effects of hydrodynamic roughness of vegetated floodplains on hydrodynamics. The roughness formulation that relates vegetation structural characteristics to a friction value has been formulated in a number of ways, (e.g. (Kouwen et al. 1969; Kouwen and Li 1980; Klopstra et al. 1997; Kouwen 2000; Järvelä 2004; Baptist et al. 2007)). None of these formulations has gained dominance in the majority of the hydrodynamic models. In the Netherlands, the WAQUA model that is used to compute water flow uses the formulation of Klopstra et al. (1997). This can be seen as a scenario uncertainty in the classification of Walker et al. (2003). In this report we will not

compare different roughness equations, but focus on the spatial variation of the model input. A few studies have investigated the sensitivity of water levels to the variation in vegetation pattern (Stolker et al. 1999; Huthoff and Augustijn 2004). Both studies use a 1D river schematization and apply arbitrary changes in vegetation pattern. No studies have been carried out using a two dimensional model, which has a better spatial representation of the roughness.

The spatial representation of the roughness is based on the ecotope map of the Rhine branches. Recently, a validation of the ecotope map has been carried out (Knotters et al. 2008), but no information is available on how errors in the ecotope map propagate through the 2D hydrodynamic model. Each of the ecotopes is assigned a value for vegetation height and density using a lookup table, which is presented in the vegetation handbook of Van Velzen et al. (2003). These lookup values are based on a limited database of field measurements, and no assessment is given on the sensitivity of the water levels to changes in the lookup table.

Our aim is to quantify the effects of two error sources:

1. classification errors in the ecotope map, and
2. errors in the lookup table,

on the following hydrodynamic aspects:

3. the discharge distribution at the bifurcation points within the river Rhine
4. peak water levels at a stationary discharge of 16000 m^3/s.

The quantification of the uncertainty in water levels and discharge distribution will help to make decisions more realistically as the error bands are substantiated. It can also influence the assessment of the height of the embankments as insight is given in the variability of the outcome of the flow models at design discharge. Moreover, the error bands may serve as an incentive to quantify the desired accuracy in the vegetation structural characteristics. This means that an upper limit can be put on the variation in water levels that is accepted from errors in the roughness parameterization. Such a choice will help the remote sensing community in setting user-defined accuracy levels instead of data driven accuracy levels. The results of this project will be of interest to an international audience, as many deltaic regions show a bifurcating river system. This research was carried out within the Flood Control 2015 program. For more information please visit http://www.floodcontrol2015.com.

2. Background

Many hydrodynamic models have been developed (see for example (Postma et al. 2000; Bates et al. 2003; Casas et al. 2006). The models may differ in (1) spatial complexity, i.e. 1D, 2D, or 3D model schematization, (2) computational grid i.e. linear, finite element, curvilinear, orthogonal, and (3) numerical solutions of the flow equations. Nevertheless, all models need data on the upstream discharge and downstream water levels as boundary conditions. River topography and hydrodynamic roughness of the main channel and adjacent floodplains complete the model input.

Accurate predictions of water levels are relevant for the height of the embankments, informing the communities on possible evacuation and for risk assessment. At this moment there is no quantification of the required accuracy of the model output. For hydrodynamic models the vegetation roughness is one of the determining factors for the computed water levels, in addition to bathymetry, roughness of the main channel and the downstream water level. The order of magnitude of the error in water level is reported in several studies. Stolker et al. (1999) modeled differences in water level using a 1D model. Assuming floodplains covered with meadows, the land cover was varied over a length of 10 km with different vegetation types and a cover percentage varying between 10 % and 100 %. Table 1 summarizes the results. For example, in case 10 % of the land cover in the floodplain is changed from meadow to reed over a 10 km stretch of river, the peak increase in water level is 15 cm. Huthoff and Augustijn (2004) reported an 8 cm change in water level and stress the effect of the shape of the cross section of the river. Both studies represent a sensitivity study as the sensitivity of the model is tested for variation in input, but they are not studies of error propagation as their input is hypothetical. Table 1 shows the results of Stolker et al. (1999).

Table 1 Effect of classification errors relative to meadows (Stolker et al. 1999)

Land cover change meadow to:	10 % changed to new vegetation cover (cm)	100 % changed to new vegetation cover (cm)
Forest and shrubs	12-20	50-120
Reed	15	50
Herbaceous vegetation	1-6	5-20

2.1 Roughness parameterization

Roughness determines the retardance of the water flow. The higher the roughness, the slower the water will flow and, hence, the higher the water levels will reach. For the non-vegetated river bed, the roughness depends on the grain size and bed form dimensions (Van Rijn 1994) . Vegetation roughness of the floodplains has been described by many different models (e.g. (Kouwen et al. 1969; Petryk and Bosmajian 1975; Kouwen and Li 1980; Dawson and Charlton 1988; Kouwen 1988; Klopstra et al. 1997; Kouwen 2000; Baptist et al. 2007)). It depends on vegetation structural characteristics like vegetation height and density, rigidity of the stems and the

presence of leaves. Vegetation density is defined as the sum of the projected plant areas in side view per unit volume (m^2m^{-3}, which reduces to m^{-1}). Seasonal variation and management that allows vegetation to vary dynamically leads to a high spatiotemporal variation of vegetation structural characteristics and inherent roughness patterns (Baptist et al. 2004; Jesse 2004; Van Stokkom et al. 2005).

Vegetation mapping using remote sensing data.
In any case the base data for roughness parameterization consists of a vegetation map of the floodplain area. Various remote sensing data may provide information on vegetation type and structure including their dynamics. Promising sensor systems include airborne laser scanning (ALS), optical systems and microwave sensors. An important issue to overcome is the translation of remote sensing information, e.g. the intensity and patterns of reflected electromagnetic radiation to relevant parameters to compute patterns of hydrodynamic roughness. Many studies reported successful and accurate mapping of natural vegetation using multispectral or hyperspectral remote sensing data (Ringrose et al. 1988; Jansen and Backx 1998; Mertes 2002; Schmidt and Skidmore 2003; Van der Sande et al. 2003). Recently, spectral information has been combined with height information in vegetation classification schemes (e.g. (Ringrose et al. 1988; Jansen and Backx 1998; Mertes 2002; Schmidt and Skidmore 2003; Van der Sande et al. 2003)). Even though the spatial resolution and the level of detail of the classification varies with the type of remote sensing data, a lookup table is always required to convert the vegetation classes to vegetation structure values, leading to the loss of within-class variation. In contrast, Airborne Laser Scanning (ALS) enables direct extraction of vegetation structural characteristics such as vegetation height, biomass, basal area, and leaf area index (Davenport et al. 2000; Cobby et al. 2001; Hopkinson et al. 2004; Straatsma and Middelkoop 2007; Straatsma 2008; Straatsma and Baptist 2008). The disadvantage of ALS being the need for vegetation calibration plots and the higher cost compared to spectral data.

Classification errors
The error matrices of these studies showed that the typical accuracy of the methods vary between 70% and 90 % and that the distinction between meadows and herbaceous vegetation is still challenging with a confusion of up to 50 %. Examples of classification accuracies include:

- Geerling et al. (2007) based on multispectral (CASI) and ALS data: 5 classes, 81 % accuracy,
- Straatsma & Baptist (2008) based on CASI and ALS data: 9 classes, 81 % accuracy,
- Van der Sande et al. (2003) using IKONOS multispectral data: 17 classes, 74 % accuracy, and
- Townsend et al. (2001) based on multitemporal Landsat multispectral data: 30 classes, 92 % accuracies, for forested wetlands, but no floodplains.

Currently the vegetation map of the lower Rhine and Meuse floodplains is based on ecotopes. Ecotopes are ‘spatial landscape units that are homogeneous as to vegetation structure, succession stage and the main abiotic factors that are relevant

to plant growth' (Van der Molen et al. 2003). Mapping of ecotopes within the lower Rhine floodplain is based on visual interpretation and manual classification of vegetation units from aerial photographs, scale 1:10,000 (Jansen and Backx 1998) . Uncertainty in classification of the terrestrial ecotopes of the Rhine branches has been determined by Knotters et al. (2008) as map purities, the percentage of the mapped area that is correctly classified. The map purity for the ecotope map of the Rhine branches of 2005 is estimated at 37% for 41 in the field distinguished different ecotopes (n=406 field observations). The overall accuracy of this map is 69% when aggregated to eight terrestrial ecotope groups (Knotters and Brus Subm.). The effects of this classification error on water level and the distribution of water over the distributaries is not known.

The quality of the validation of the ecotope map has been evaluated in Houkes (2008). The following discrepancies were noted:

- The smallest mappable unit in the field was smaller than on the ecotope map, leading to within class variation labelled as differences in ecotopes. This contributes to a lower classification error as the spatial support differs between the field observation and the map.
- A number of characteristics of the ecotope interpretation key are not discernable in the field, leading to errors in the field observation. However in the validation, the field data were used as if they were error free.
- Some positioning errors were made in the field.

The combined effect of these flaws in the validation might lead to an underestimation of the accuracy of the ecotope map. Other studies showed higher accuracies and the effects on the hydrodynamics should therefore be seen as a maximum variation.

Errors in lookup tables

Contrary to the classification accuracy, the error in the lookup table is not well-known. Popular guidelines on selecting roughness values e.g. (Chow 1959; Arcement and Schneider 1989) give Manning's values, without taking the water depth into account, and only make a weak link to vegetation structure. Van Velzen et al. (2003) provided a complete lookup table with all the relevant vegetation parameters. They also provide a list of field reference sites and their measured vegetation structure for each vegetation class. It is clear from this list that the variation in vegetation structure is large and that only few measurements are available. The error in the lookup table is therefore largely unknown.

2.2 Roughness parameterization in WAQUA

The implementation of roughness in hydrodynamic models varies. For WAQUA, the required data for model input has been made available by the Ministry of Public Works, Transport and Water Management (RWS, 2008) in the Baseline 4.03 database (Hartman and Van den Braak 2007). It contains a complete dataset of base maps, derived maps, and a model schematization for the Rhine branches. The

hydrodynamic roughness is implemented in a very detailed form in the Baseline database. For WAQUA, hydrodynamic roughness is derived from point, line, and polygon information (Fig. 1).

Roughness polygons are derived from the ecotope map, which is combined with the outline of the main channel, lakes and high water free areas. All these maps are converted using a lookup table to determine the roughness-polygon map (Fig. 1). Each roughness code for vegetation is linked to vegetation structural parameters, such as vegetation height and density plus bottom roughness and drag (Van Velzen et al. 2003). The roughness in the WAQUA model, expressed as Chézy C, depends on the water depth and is computed during runtime of the model using the equation presented in Klopstra et al. (1997). The roughness is assigned to the model computational cell and the energy loss is computed over the cell.

Point and line elements of roughness are derived from a database containing hedges, individual trees and tree-lined lanes. These files are compiled in the Digital Topographic Dataset of the wet infrastructure (DTB-nat) and lead to more detail in the roughness parameterization. Hedges are parameterized as line elements, assigned with a height and a density, whereas single trees are represented as point data with tree diameter as relevant hydrodynamic parameter. The energy loss of these roughness elements is computed, and attributed to the cell boundary containing the roughness elements.

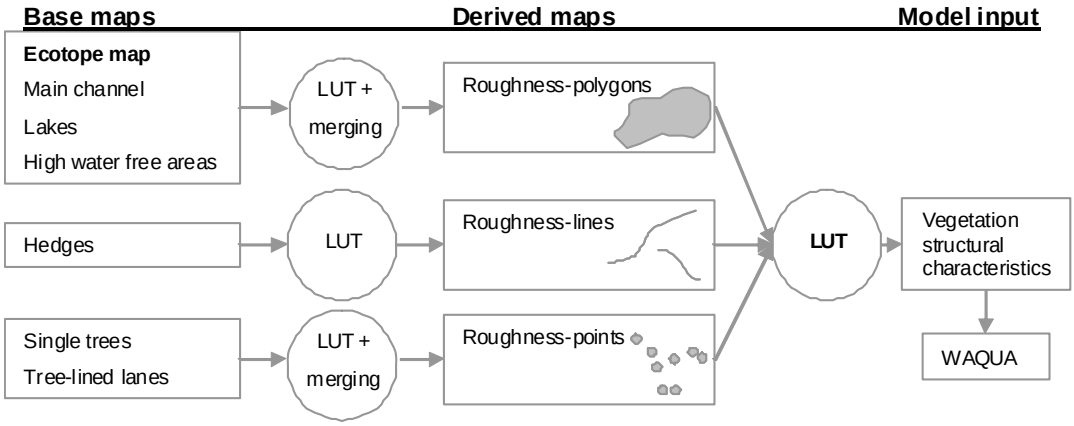

Figure 1. Flow chart of roughness parameterization for the WAQUA hydrodynamic model. The elements that were varied in this study are printed in bold, all other sources of roughness input have been kept constant. The vegetated ecotopes have been varied according to the classification accuracy table (Knotters et al. 2008). The lookup table (LUT) relating the derived maps to the WAQUA input has been changed based on field measurements.

3 Study area

Within this study, we looked at the distributaries of the river Rhine in the Netherlands, excluding the estuary. At the Dutch-German border, the river Rhine has an average discharge of 2250 m^3/s, draining a catchment area of 165 000 km^2. Coming from Germany, the river Rhine bifurcates into the "Pannerdensch Kanaal" and the Waal river at the "Pannerdensche Kop" (PK) bifurcation point where roughly one third enters the "Pannerdensch Kanaal" and two thirds are conveyed into the river Waal. At the "IJsselkop" (IJK) bifurcation point again, one third enters the right hand channel named the IJssel river and two thirds flow into the Nederrijn river (Fig. 2). However the exact ratio of dividing the water over the channels depends on the shape and roughness of the main channel and the floodplain.

The study area spans three distributaries with an average water gradient of 0.10 m/km and a maximum length of 152 km along the river axis, which is for the IJssel. The total embanked area amounts to 440 km^2, the floodplain area is 320 km^2 out of which 48 km^2 consists of lakes and side channels. The vegetated area takes up 62 % of the total embanked area. Groynes fixate the main channel and limit the width of the main channel to 250, 160, 105 m for the Waal, Nederrijn and IJssel river. The cross-sectional width between the primary embankments varies between 0.5 and 2.6 km. Meadows dominate the land cover, but recent nature rehabilitation programs led to increased areas with herbaceous vegetation, shrubs and forest.

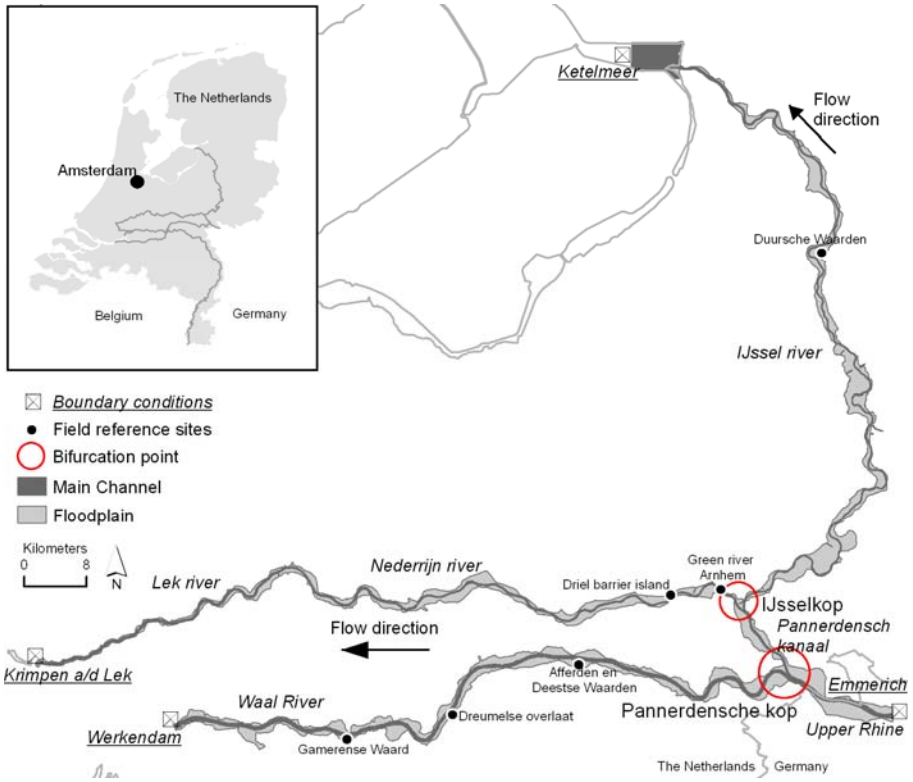

Figure 2 Study area showing the three main distributaries of the river Rhine; Waal, Nederrijn/Lek and IJssel river. At the bifurcation points "Pannerdensche Kop" and "IJsselkop" the water is distributed over the three branches.

4 Methods

In this sensitivity analysis, we focused on two aspects of the roughness parameterization and the error propagation in the hydrodynamic model. Firstly the effect of classification errors was assessed and secondly the sensitivity to errors in the lookup table that relates roughness codes to vegetation structural characteristics like height and density. Both aspects have been highlighted in figure 1. The resulting error in the water level prediction is normally limited in a subsequent step of calibration. Due to the limited scope of the present study this calibration has been omitted, and the results should therefore not be interpreted as possible water level variations during the design discharge.

The roughness polygons are changed based on the ecotope map of 1997 (Jansen and Backx 1998) as used in the BASELINE 4.03 dataset, and the classification accuracy table of Knotters et al. (2008). This will provide information on the classification error. Line elements and point elements have not been changed. In addition, the roughness lookup table containing the vegetation structural parameters has been varied showcasing the sensitivity to an error in vegetation structural parameters, i.e. vegetation height and density. The range of values has been based on the available field inventory data of the last 10 years.

4.1 Propagation of classification errors

At the base of this analysis lies the validation of the ecotope maps by Knotters et al. (2008), and the ecotope map of Jansen and Backx (1998). For each ecotope, the table with map purities shows the area of the map that is classified correctly, and the area that is classified as another class. Correct classification is found on the diagonal of the matrix, erroneous areas are given on the other cells on each row (Table 2). In total the map purities per row sum up to one. Table 2 shows a simplified example of a map purities table. In this research, we use the map purities table as probabilities that an ecotope polygon is classified correctly, assuming similar size for the polygons. For example, the ecotope forest has a probability of 0.70 of correct classification, but is classified as meadow with a probability of 0.17.

For each ecotope polygon, we created 30 new realizations based on the probabilities given in the table of map purities. To that end we generated a random number between zero and one based on a uniform distribution. Based on the cumulative sum per ecotope, a new ecotope code was assigned to each polygon in the ecotope map. Figure 3 illustrates the assignment of new ecotope codes. For a random number of 0.2 (indicated by the red dashed line), meadow would remain meadow, herbaceous would change to meadow and forest would be converted to herbaceous vegetation. For forest it means that the resulting polygon would be labeled as forest around 21 times (0.70 *30), 5 times as meadow, and around 4 times as herbaceous. This procedure was carried out for each individual polygon and for each variation. All of these maps have the same probability and can be seen as different outcomes of the same manual ecotope map.

Table 2. Simplified and fictitious example of the map purities with the cumulative sum per row in brackets.

	Field observation		
Map	**meadow**	**herbaceous**	**forest**
meadow	0.60 (0.60)	0.35 (0.95)	0.05 (1.00)
herbaceous	0.30 (0.30)	0.50 (0.80)	0.20 (1.00)
Forest	0.17 (0.17)	0.13 (0.30)	0.70 (1.00)

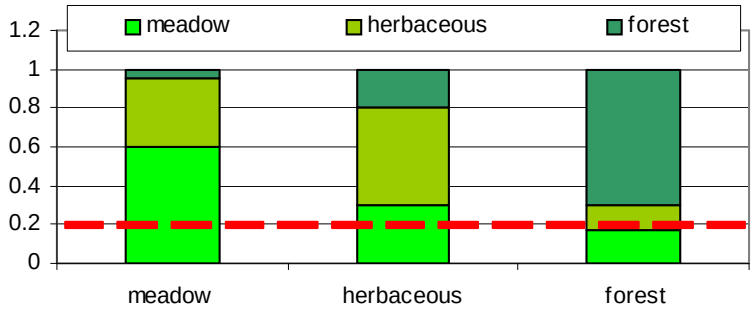

Figure 3 Cumulative values of map purities based on values of table 1. Based on a random number between 0 and 1, the new class is assigned to that polygon.

The real situation is more complicated. Knotters et al. (2008) carried out the validation of the ecotope maps of the Rhine distributaries based on 406 field observations. This table is give in appendix A. We made a number of adjustments to this table because:

1. the field data were not collected based on the same legend as the ecotope map, as some ecotopes were indiscernible in the field,
2. not all ecotopes were present in the field area used for validation,
3. only terrestrial ecotopes were validated.

The description of the codes of the ecotopes are given in Appendix A. The first step was to standardize the rows and columns of the map purity table of Knotters et al. (2008) into the same ecotope codes. The following adjustments were made:

1. The field code HK2 does not exist in the ecotope classification. The column has been joined with HK1.
2. HK1 is an older code, used until 2004, and represents bare areas at higher elevation. This can not be due to morphodynamics and therefore must be the result of human interference. DID decided to recode this class to HREST, other types of bare earth.

3. A number of codes were renamed as the distinction between floodplains ("U") and levee ("O") is not made any more since the second ecotope mapping:
    1. OA-2 to O-UA-2,
    2. OB-1 to O-UB-1,
    3. OB2 to O-UB2,
    4. OB-4 to O-UB-3,
    5. OG1 to O-UG-1,
    6. OG2 to O-UG-2,
    7. OK1 to O-UK1,
    8. OR-1 to O-UR1.
4. UR-1-2 was combined with UR-1
5. IV.1-2 was combined with IV.8-9. Both represent reed. IV.1-2 does not occur on the map.
6. OB-2 and OB-4 were summed and assigned to O-UB-2. The class "thorny shrubs on levees" (OB-4) has expired.
7. All classes starting with O have been replaced by O-U.
8. O-UG-1 and O-UG-1-2 have been joined.
9. VI.1 (grey willow shrubs) were added to VI.2 (softwood shrubs) to create the class VI.1-2.

It should be noted that these changes were needed to enable the implementation, but do not reflect the flaws in the validation that were listed in section 2.1.

The second step consisted of adding the water ecotopes to complete all the possible ecotopes that occur in the Rhine distributaries. These ecotopes were not part of the validation, nor were they changed in this study. All the water ecotopes were therefore assigned a value of one on the diagonal of the map purities table, see Appendix B. The last step was to add the terrestrial ecotopes that were not present in the validation data set. An informed, but arbitrary choice was made for the errors for this class. The error distribution mimics the error distribution of similar ecotopes. These rows and columns have been highlighted in yellow in Appendix B.

4.2 Errors in vegetation structural characteristics

Even though ecotopes are considered homogeneous as to vegetation structure in the definition, field measurements have shown that ecotopes are far from homogeneous with respect to vegetation structure (Straatsma and Ritzen 2002). For this study field reference data have been compiled of studies carried out by eight studies (Asselman 2002; Straatsma and Ritzen 2002; Straatsma and Middelkoop 2007; Warmink 2007; Amoureus and Bomers 2008; Straatsma 2008; Straatsma et al. 2008; Straatsma 2009). The original data was not always reported in full detail in these studies. The field measurements have now been standardized and were combined into a database containing the location, date, field workers, ecotope codes, roughness codes, method and structural information on vegetation height and density. The data in this database have not been collected using a purposive sampling strategy aiming at the full coverage of all vegetation types of Van Velzen et al. (2003). Some of the types are not sampled in detail, or the ecotope map does not

represent the local detail in the vegetation. Therefore, omissions are present for some types. To be able to estimate the error for all vegetation types, the values of the vegetation handbook of Van Velzen et al. (2003) have been used and changed based on our own expert judgment. The variation in vegetation structure has been summarized per roughness class for the winter situation. Winter time is the most likely period of flooding in the Netherlands, the variation of vegetation height and density over the year has been ignored. Variation in vegetation structure was characterized by the 0^{th}, 25^{th}, 50^{th}, 75^{th}, and 100^{th} percentile of the distribution of vegetation height and separately for vegetation density.

4.3 Modeling

The WAQUA model has been used by the Dutch Ministry of Transport, Public Works and Water Management for the two-dimensional simulation of hydrodynamics in the complex channel and floodplain areas of the Rivers Rhine and Meuse in the Netherlands (RWS 2007). For the present study, a series of simulations of steady flow in the study area was carried out. The WAQUA model that was used for this study is based on a staggered curvilinear grid. Each of the 886,861 cells represents a column shaped volume of water with a variable surface area of 1000 m^2 on average. The water flow between the water volumes in the raster is calculated by numerically solving the Saint-Venant equations of mass balance and of convective and diffusive motion in two dimensions (RWS 2007) using a finite difference method. The boundary conditions of the model are the river discharge at the upstream boundary, and the water level at the downstream boundary using a discharge-stage relationship. Input data from which the WAQUA model calculates the water flow field are a Digital Terrain Model (DTM), barriers and a roughness map. We ran WAQUA with a discharge of 16,000 m^3/s at the upstream end at Emmerich, Germany. Water levels at the downstream end were around 4.39, 2.02 and 0.42 m above ordnance datum for the downstream boundary conditions of the Waal, Nederrijn-Lek and IJssel rivers respectively. The full model of the Rhine branches was run as proximity of the boundaries to the bifurcation points would limit the effect of water level variations.

We ran two sets of model runs. The first set consisted of 15 model runs with different ecotope maps as input. The number of model runs was limited as the time required for individual runs amounted to eleven hours or more on a computational cluster of 10 processors. The second set consisted of five runs with different values for vegetation structural characteristics based on the available field data. Values chosen were the minimum, 25-percentile, median, 75-percentile and maximum for vegetation height and density. Output of these model runs are evaluated with respect to the changes on the water levels on the river axis, and water distribution over the bifurcation points.

5. Results

In this section we present examples of the ecotope map realizations, and the variation of vegetation structure per vegetation type (section 5.1 and 5.2). In section 6.3, and 5.4 we present the effects on the flow characteristics.

5.1 Classification error

An example of different realizations of the ecotope map based on the classification error are given in figure 4. It shows two realizations of the ecotope distribution around the bifurcation points. Ecotopes have been aggregated to the vegetation types that are distinguished by Van Velzen (2003). The detail of the Millinger Waard floodplain section indicates the variation per polygon. The large field on the upstream end is classified as natural grass and hayland in run 1 and as production meadow in run 5. Other variations include changes from shrubs to forest and from agriculture to meadows. At ecotope level few ecotopes maintain their classification as the map purity is around 25 percent. At the aggregation level of vegetation types (Fig. 4) the probability for maintaining the same class is higher, because the probabilities of the low level classes are summed. Note that the water bodies have not changed. In appendix C the full error matrix is give that lies at the base of the different realizations.

5.2 Overview of vegetation structural characteristics for the Rhine branches

The compilation of the field data resulted in a database of 445 field measurements, 189 of these were taken during leaf-off season. For 17 measurements of forest the summer measurements are also representative of the winter situation as the vegetation density of the stems does not change between the seasons. The reference data were distributed over six floodplain sections: (Fig. 1). Especially the Gamerense Waard, the Duursche Waarden and the Afferden en Deestse Waarden display a wide variety of vegetation types as these floodplain sections are managed by nature conservation organizations.

The variation in the field reference data per vegetation type has been summarized in table 4 by the 0, 25, 50, 75, and 100 percentile of the vegetation height and density. The values printed as normal font are based on field measurements, the values in bold are derived from Van Velzen (2003). The percentiles for the vegetation types that were based on the vegetation handbook were based on our own expert judgment. It is clear that the table is not complete with only half of the entries based on a substantial number of field measurements. This is caused by the original purpose of the field campaigns that was not meant for linking with the vegetation handbook. Especially the different herbaceous classes were not well differentiated.

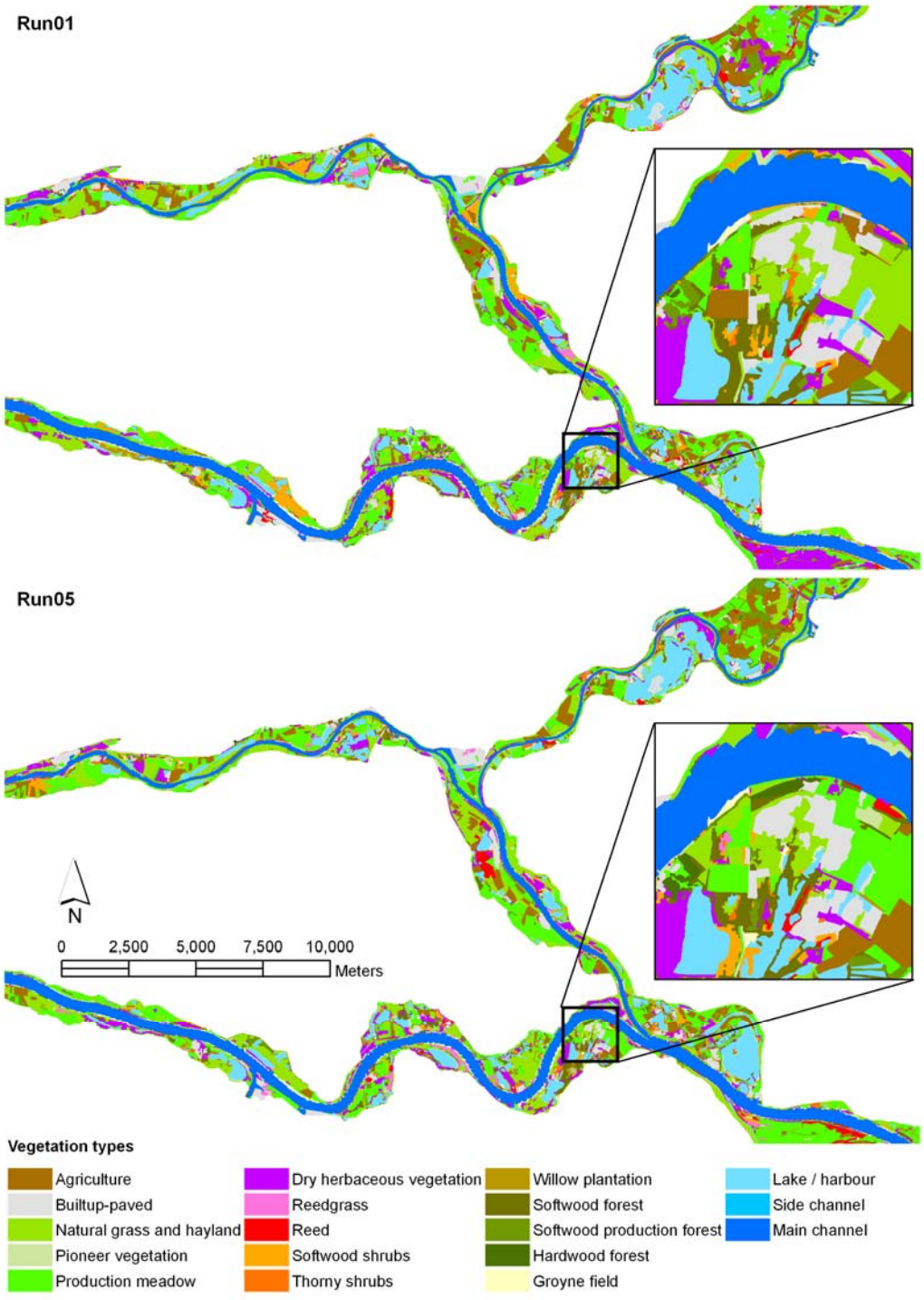

Figure 4. Example of two out of the thirty ecotope maps that were generated based on the current ecotope map of the whole study area and the map purities table of Knotters et al. (2008). Ecotopes have been aggregated to the level of vegetation types to limit the number of classes for visual inspection. Large differences in vegetation type assignment are visible. The detail gives the situation for the Millinger Waard floodplain section.

Remarkable differences become apparent between the field data and the current lookup table of the vegetation handbook for the classes that were well sampled in the field. For example softwood and hardwood forest are 50% more dense according to the field data, the density of production meadow is at 20% percent of the current value, natural grass and hayland is higher and less dense compared to the handbook data. Vegetation structure varies strongly for some vegetation types. A dense softwood forest may be 30 times more dense than an open area of softwood forest. For reed-grass, dry herbaceous vegetation, and softwood shrubs, the lowest value may be a factor between 10 and 20 more open than the highest value. Variation in vegetation height is especially high for natural grass and hayland.

Table 3 Attributes of the 445 field data points collected between 2000 and 2007.

Attribute	Description
Point.no	Original sequential point number in the original data
Floodplain	Floodplain section
Institute	Leading institute in the project
Field workers	Field workers
Report	Name of the report using the data
Date	Date of field data collection
Season	Summer / winter
Xcoor	Northing in RD, the dutch projection system
Ycoor	Easting in RD, the dutch projection system
Ecocode1	Ecotope code of the first ecotope mapping cycle (1997)
Ecocode2	Ecotope code of the second ecotope mapping cycle (2003)
Veg type	Handbook type (Van Velzen et al. 2003) based on field info
Dbh	Diameter at breast height, or at half the vegetation height for herbs
N	Number of stems per m^2
Dvmeten	Vegetation density based on the product of N and dbh
Method	Manual or photographic method
Remarks	Additional informtion
CodeB4Eco1	Baseline 4 code based on the first ecotope mapping cycle
CodeB4Eco2	Baseline 4 code based on the second ecotope mapping cycle
Handbook1	Vegetation type based on CodeB4Eco1
Handbook2	Vegetation type based on CodeB4Eco2

* Dv = vegetation density (m^2/m^3) , Hv = vegetation height (m)

Table 4. Summary of the 206 relevant field reference points of the complete database of 445 vegetation measurements. For each of the vegetation types of Van Velzen et al. (2003) the 0, 25, 50 75 and 100 percent percentile have been computed when enough data was available, otherwise a best guess of these values is given (printed in bold). These values were put in the rough.karak_hr2006 file in the Baseline tree.

Code	Class	Vegetation handbook	0%	25%	50%	75%	100%	N
Vegetation density (m^{-1})								
1201	Production meadow	**45**	**1.00**	**6.00**	**12.00**	**18.00**	**40.00**	1
1202	Natural grass and hayland	**12**	0.020	0.027	0.077	0.134	0.350	29
1203	**Herbaceous meadow**	**15**	**3.00**	**10.00**	**15.00**	**16.00**	**20.00**	**NA**
1211	**Thistle herb. Veg.**	**3**	**1.00**	**2.00**	**3.00**	**4.00**	**5.00**	**NA**
1212	Dry herbaceous vegetation	**0.23**	0.011	0.030	0.047	0.073	0.219	16
1213	**Brambles**	**0.56**	**0.100**	**0.350**	**0.560**	**0.600**	**0.700**	**NA**
1214	**Hairy willowherb**	**0.13**	**0.150**	**0.500**	**0.950**	**1.100**	**1.250**	**NA**
1215	**Reed herb. Veg.**	**0.16**	**0.100**	**0.130**	**0.160**	**0.200**	**0.250**	**NA**
1221	**Wet herb. Veg.**	**0.25**	**0.100**	**0.150**	**0.250**	**0.300**	**0.400**	**NA**
1222	**Sedge**	**1.2**	**0.012**	**0.600**	**1.200**	**1.800**	**2.000**	**NA**
1223	Reed-grass	**0.4**	0.088	0.099	0.111	0.129	0.147	3
1224	Bulrush	**1.2**	**0.012**	**0.600**	**1.200**	**1.800**	**2.000**	**NA**
1225	**Reed-mace**	**0.35**	**0.100**	**0.200**	**0.350**	**0.500**	**0.700**	**NA**
1226	Reed	**0.37**	0.122	0.226	0.338	0.456	0.544	6
1231	Softwood shrubs	**0.13**	0.025	0.057	0.121	0.198	0.354	26
1232	**Willow plantation**	**0.041**	**0.005**	**0.025**	**0.041**	**0.060**	**0.120**	**NA**
1233	Thorny shrubs	**0.17**	**0.100**	**0.130**	**0.170**	**0.250**	**0.400**	**NA**
1241	Hardwood production forest	**0.011**	**0.002**	**0.005**	**0.011**	**0.015**	**0.020**	**NA**
1242	Softwood production forest	**0.01**	**0.002**	**0.005**	**0.010**	**0.015**	**0.020**	**NA**
1243	Pine forest	**0.016**	**0.005**	**0.010**	**0.016**	**0.025**	**0.030**	**NA**
1244	Hardwood forest	**0.023**	0.001	0.018	0.034	0.050	0.364	66
1245	Softwood forest	**0.028**	0.008	0.023	0.047	0.105	0.246	41
1246	**Orchard low**	**0.024**	**0.016**	**0.020**	**0.024**	**0.030**	**0.035**	**NA**
1247	**Orchard high**	**0.01**	**0.008**	**0.009**	**0.010**	**0.011**	**0.012**	**NA**
1250	**Pioneer vegetation**	**0.15**	**0.050**	**0.100**	**0.150**	**0.200**	**0.400**	**NA**
Vegetation height (m)								
1201	Production meadow	**0.06**	0.02	0.03	0.04	0.06	0.16	27
1202	Natural grass and hayland	**0.1**	0.05	0.34	0.46	0.71	1.34	32
1203	**Herbaceous meadow**	**0.2**	**0.10**	**0.15**	**0.20**	**0.25**	**0.30**	**NA**
1211	**Thistle herb. Veg.**	**0.3**	**0.15**	**0.20**	**0.30**	**0.35**	**0.40**	**NA**
1212	Dry herbaceous vegetation	**0.56**	0.04	0.42	0.57	0.71	1.43	19
1213	**Brambles**	**0.5**	**0.35**	**0.45**	**0.50**	**0.60**	**0.90**	**NA**
1214	**Hairy willowherb**	**0.95**	**0.08**	**0.10**	**0.13**	**0.25**	**1.30**	**NA**
1215	**Reed herb. Veg.**	**2**	**1.00**	**1.50**	**2.00**	**2.10**	**2.30**	**NA**
1221	**Wet herb. Veg.**	**0.35**	**0.15**	**0.25**	**0.35**	**0.45**	**0.60**	**NA**
1222	Sedge	**0.3**	**0.03**	**0.15**	**0.30**	**0.45**	**0.60**	**NA**
1223	Reed-grass	**1**	0.05	0.21	0.41	0.78	1.49	4
1224	Bulrush	**0.5**	**0.05**	**0.25**	**0.50**	**0.75**	**1.00**	**NA**
1225	**Reed-mace**	**1.5**	**0.80**	**1.20**	**1.50**	**1.70**	**2.00**	**NA**
1226	Reed	**2.5**	2.05	2.28	2.56	2.85	3.12	4
1231	Softwood shrubs	**6**	3.20	5.25	6.00	7.20	12.00	14
1232	**Willow plantation**	**3**	**1.00**	**2.00**	**3.00**	**4.00**	**5.00**	**Na**
1233	Thorny shrubs	**5**	**1.00**	**2.50**	**5.00**	**7.50**	**9.00**	**NA**
1246	**Orchard Low**	**3**	**2.50**	**2.75**	**3.00**	**3.25**	**3.50**	**NA**
1247	**Orchard high**	**6**	**3.00**	**5.00**	**6.00**	**7.00**	**8.00**	**NA**
1250	Pioneer vegetation	**0.15**	0.01	0.05	0.06	0.06	0.12	6

5.3 Hydrodynamic effects of classification errors

The effect of classification errors on the discharge distribution and water levels was assessed using 15 model runs of the Rhine branches. Each of the runs used the same boundary conditions.

Flow pattern
The classification errors had clear effects on the flow pattern. Figure 5 shows the differences between run eco01 and eco05 for water levels and flow velocities. For example in the north of the Millinger Waard floodplain section, enlarged on the detail in the figure, the vegetation on the bank of the river is meadow, and paved in run05 and softwood shrubs in run01 (Fig. 4). This leads to higher flow velocities and lower water levels.

Discharge distribution
The average effect on the discharge distribution is a variability of 170, 163, 155, and 163 m^3/s for the Waal, Pannerdensch Kanaal, Nederrijn and IJssel river respectively (Table 5). This is around 1 % of the total discharge of 16000 m^3/s routed through the distributaries. Even though the fraction of water conveyed to each river branch does not vary much resulting from the different realizations, the changes in water level at 16000 m^3/s are not negligible (Fig. 6). Differences of up to 4.5 cm may in water level may result from the variation of discharge distribution.

Water levels
Water levels vary due to the different ecotope input maps. We show the effect of the different roughness maps on the water levels at the axes of the rivers. Figure 7 gives the outcome of the individual runs. Data has been summarized for the following river sections: (1) Bovenrijn-Waal (BRWA), (2) Pannerdensch Kanaal-Nederrijn-Lek (PKNELE), and (3) IJssel (IJ). The variation is summarized by the range and standard deviation in water levels for each river kilometer at the river axes. The maximum range in water levels is 0.40, 0.40 and 0.57 m for BRWA, PKNELE and IJ respectively. The larger range for the IJssel river results from the large fractional discharge at this distributary. The outcome of the individual model runs is shown as thin grey lines. A spatial overview of the range in water levels is given in figure 8, which also gives the river kilometers for spatial reference with figure 7. Note that the variation at the model boundaries is limited due to the applied discharge-water level relationship. The variation of the water level at the boundaries resulted purely from the variation in discharge.

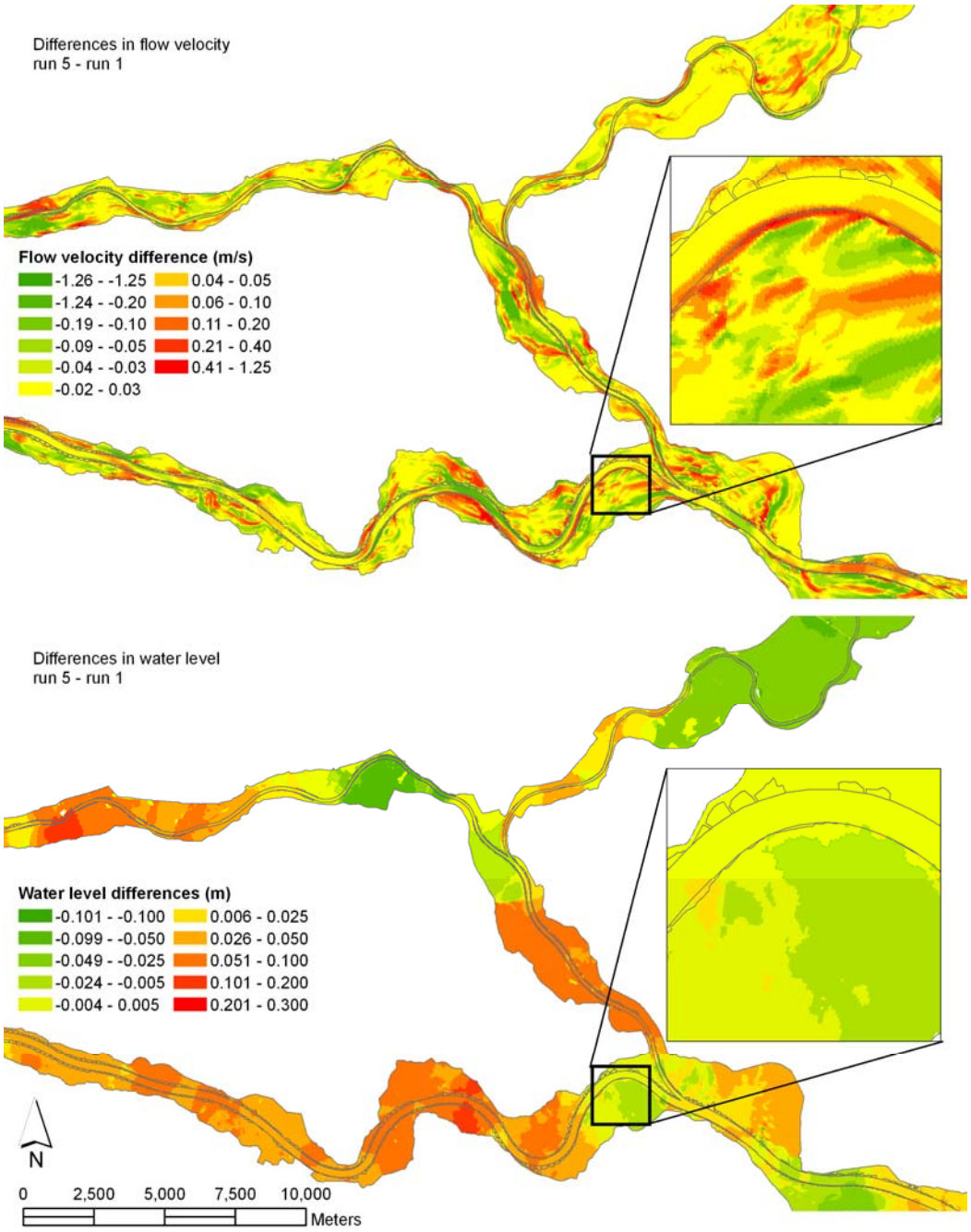

Figure 5. Differences between two out of 15 model runs.
The discharge distribution at the Pannerdensche Kop bifurcation point varies due to the errors in classification. The standard deviation of the discharge for all distributaries is around 25 m^3/s, the range in the variation is up to 170 m^3/s for the Nederrijn distributary. This variation is around 1 % of the total discharge of 16,000 m^3/s. Table 5 gives the details of the individual runs.

Table 5. Effect of classification errors on the discharge distribution of water over the various branches of the river Rhine. The range in discharge variation of maximum 163 m^3/s leads to a 5 cm maximum variation in water level (Fig. 6)

	Discharge (m^3/s)				Fraction (-)			
Run no.	**Waal**	**Pan. kanaal**	**Nederrijn**	**IJssel**	**Waal**	**Pan. Kanaal**	**Nederrijn**	**IJssel**
eco00	10086	5917	3336	2585	0.630	0.370	0.208	0.162
eco02	10090	5907	3344	2567	0.631	0.369	0.209	0.160
eco03	10037	5967	3389	2582	0.627	0.373	0.212	0.161
eco04	10078	5920	3312	2610	0.630	0.370	0.207	0.163
eco05	10077	5928	3323	2605	0.630	0.371	0.208	0.163
eco06	10049	5950	3355	2597	0.628	0.372	0.210	0.162
eco08	10030	5980	3318	2663	0.627	0.374	0.208	0.167
eco09	10056	5947	3234	2713	0.629	0.372	0.202	0.170
eco10	9989	6008	3374	2638	0.624	0.375	0.211	0.165
eco11	10150	5858	3285	2575	0.635	0.366	0.206	0.161
eco13	10064	5942	3370	2569	0.629	0.371	0.211	0.161
eco14	9994	6011	3363	2649	0.625	0.376	0.210	0.166
eco15	9980	6021	3294	2730	0.624	0.376	0.206	0.171
Range	**170**	**163**	**155**	**163**				
St. dev.	**47**	**47**	**43**	**54**				

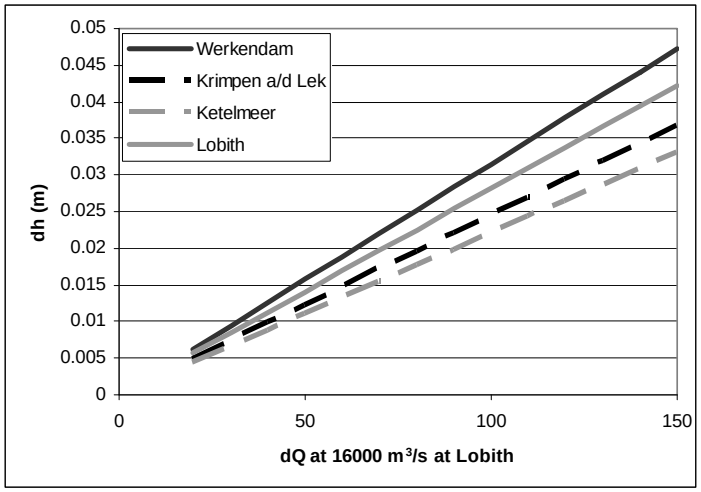

Figure 6. Relationship between changes in discharge at design discharge, 16000 m^3/s and changes in water level at Lobith and the downstream model boundaries Werkendam, Krimpen a/d Lek and Ketelmeer.

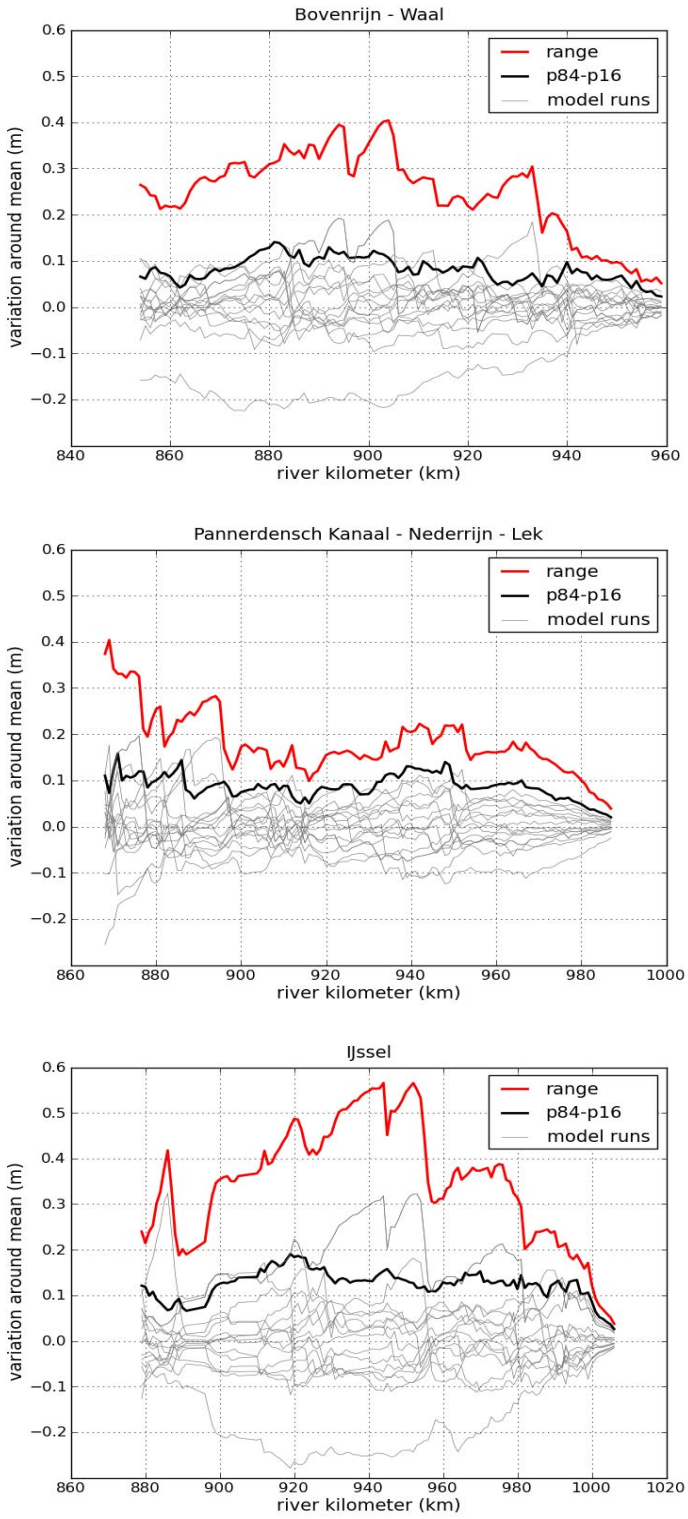

Figure 7. Overview of water level variation due to error in classification of the ecotope map. The largest variation is seen on the river IJssel, 0.57 m.

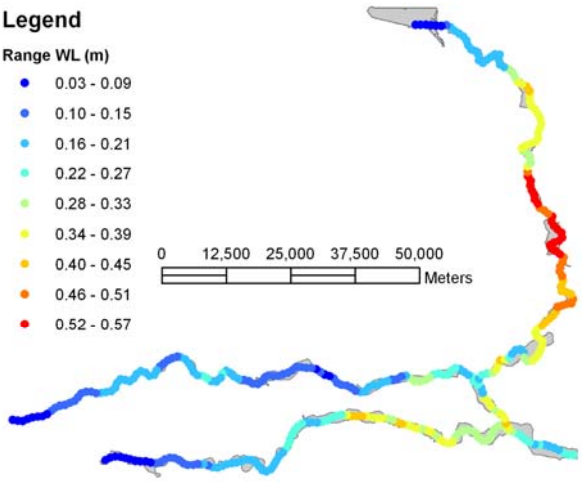

Figure 8. Range of variation in water levels per river kilometer (differences with current ecotope map) due to different realizations of the ecotope map. Largest values are found on the IJssel river.

Number of runs

In the current study the number of individual runs was limited to 15. Initially, the number of ecotope realizations was set to thirty, but the computational demands of the WAQUA model of the Rhine branches are large. Therefore the number of model runs was limited to 15. No time was available within the project to do additional runs. The questions rises whether enough runs were done to reliably estimate the range in expected water levels. We addressed this issue by plotting the number of runs against the measured variation per river branch (Fig. 9). Note that this figure gives the range per river branche, whereas the values in figures 7 and 8 are per river kilometer, thus generating different values. It is clear that the variation in range and standard deviation stabilizes around 10 model runs, but the twelfth run was again an exceptional distribution of ecotopes leading to an even higher range for the Waal and IJssel river.

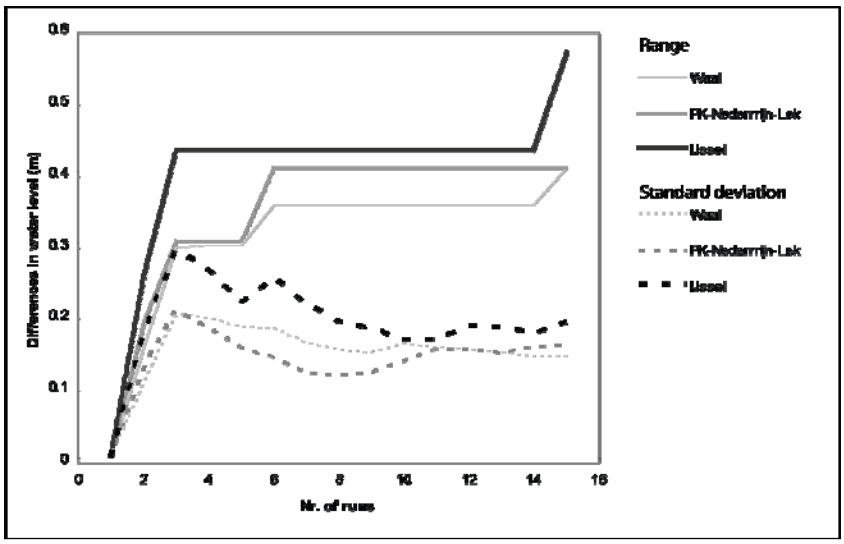

Figure 9. Relationship between the number of model runs and the range and standard deviation computed over all the river kilometers per section Variation tapers off around 10 model runs, but run number 15 (eco15) was an extreme case with high water levels especially in the river IJssel.

5.4 Hydrodynamic effects of errors in structural characteristics of vegetation

The discharge distribution varies with the values in the lookup table as well (Table 6). Especially the distribution at the Pannerdensche Kop varies strongly. A change from the median values of vegetation height and density to the 25th and 75th percentile leads to a 150 m^3/s change in discharge for the Waal and Pannerdensch Kanaal.

The sensitivity of the water levels for changes in structural characteristics as listed in the lookup table given in Fig. 10. The range in values is larger than for the error in the ecotope map. The range rises to than one meter for the IJssel river. The range in values should be considered an extreme as for the 0 and 100 percentile input data, the maximum for both the vegetation height and density is used, whereas in real life these value are negatively correlated. Higher vegetation is generally more open. The interquartile range is more realistic. The interquartile range, difference between the 75 and 25 percentile is 0.20, 0.25 and 0.36 m for the BRWA, PKNELE and IJ river sections respectively (Fig. 10).

Table 6. Effect of changes in vegetation structural characteristics on the discharge distribution of water over the various branches of the river Rhine.

	Discharge				Fraction			
Run no.	**Waal**	**Pan. kanaal**	**Nederrijn**	**IJssel**	**Waal**	**Pan. Kanaal**	**Nederrijn**	**IJssel**
eco00	10086	5917	3336	2585	0.630	0.370	0.208	0.162
LUT000	10215	5790	3352	2433	0.638	0.362	0.209	0.152
LUT025	10107	5911	3398	2511	0.632	0.369	0.212	0.157
LUT050	10010	5995	3439	2556	0.626	0.375	0.215	0.160
LUT075	9949	6059	3470	2589	0.622	0.379	0.217	0.162
LUT100	9856	6149	3491	2659	0.616	0.384	0.218	0.166
IQR[a]	**-158**	**148**	**72**	**78**				
Range	**359**	**359**	**155**	**225**				
St. dev.	**127**	**126**	**63**	**77**				

[a] IQR = interquartile range

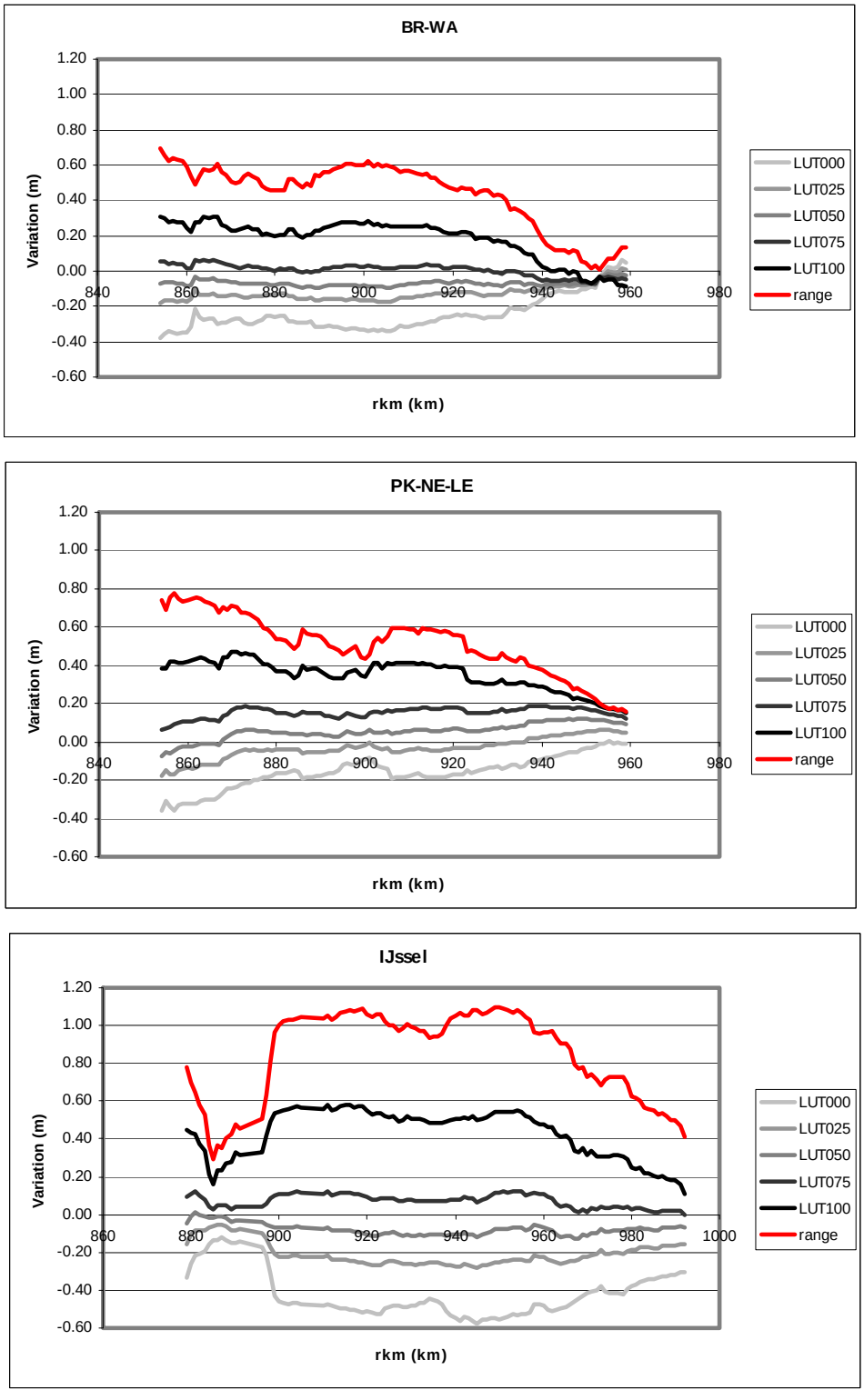

Figure 10. Variation of water levels for three river sections BRWA, PKNELE, and IJ based on the values in the lookup table (Table 3) The differences are given relative to the current values in the vegetation handbook. See figure 8 for the location of the river kilometers (rkm). Range shows the difference between the minimum and maximum water level at that river kilometer.

6. Discussion

In the previous section, we looked at the hydrodynamic effects due to classification errors and the sensitivity for structural characteristics in the lookup table. In general the effects are relatively large when compared to the accuracy required for the hydraulic boundary conditions. For landscaping measures the effect should be less than 2 mm rise in water level at the river axis and less than 5 m^3/s change in discharge distribution over the bifurcation points (RWS 2008). The results show that the hydrodynamics are strongly related to the spatial roughness parameterization. The results should not be interpreted as absolute errors in the prediction, nor as the required increase in the height of the embankment, as the calibration has not been repeated for each variation. Repeated calibration is very time consuming. Still it would be desirable to have this absolute variation in water levels at the design discharge due to floodplain roughness. When the other sources of error are quantified as well, a probabilistic approach can be followed to determine the required height and strength of the embankments.

Comparison between error sources
The variation in water levels from different realizations of the ecotope map amounts to 0.40, 0.40 and 0.57 m for Upper Rhine- Waal, Pannerdensch Kanaal-Nederrijn-Lek and the IJssel river respectively (Fig. 7) . To compare these values to the error based on the lookup table we have to take a realistic value. The range in values for both vegetation height and density gives the most extreme case, but in reality these parameters are negatively correlated. A high vegetation height comes with a lower density. The interquartile range is considered more realistic. Therefore, we will compare the results from the interquartile range from the lookup table to the results from the classification error. The interquartile range of the LUT gives a range of water level differences of 0.2, 0.2, and 0.36 m Upper Rhine- Waal, Pannerdensch Kanaal-Nederrijn-Lek and the IJssel river respectively (Fig. 10). This suggests that the classification accuracy is more important than more correct values in the lookup table.

With respect to the discharge distribution, the effects of the two error sources is similar for the distribution at the Pannderdensche Kop bifurcation point. For the lookup table error, we use the interquartile range again. Both error sources result in a variation of around 165 m^3/s. At the IJsselkop bifurcation point the error from the lookup table gives a weaker variation than the error from the ecotope classification. Compare tables 4 and 5 for details. Also in this case, the priority should be with improving the classification error when the variation in water levels is to be limited.

Classification error and variation in water levels
Another implication of the error propagation of the classification error is that a relation could be established between the classification accuracy and the variation in

water levels. In the present study we linked a 69 % classification accuracy to a maximum range in water levels is 0.40, 0.40 and 0.57 m for BRWA, PKNELE and IJ respectively. However the accuracy level of the classification has been disputed. Flaws in the field validation were related to (1) a small support for the field observations leading to the classification of within class variation as different ecotopen, (2) morphodynamics and inundation duration are difficult to discern in the field from biotic information, and (3) fuzzy boundaries between classes. The correct accuracie might therefore be higher, and the differences in water level subsequently smaller.

For a higher classification accuracy the variation in water levels will be smaller as more of the polygons will maintain their class. Based on such a relation a political choice can be made about the accepted amount of uncertainty that the river manager is willing to allow for the water levels. This uncertainty in water levels can than be translated into a classification accuracy. A tangible benchmark for classification accuracy that is substantiated by research would be a stimulation for the remote sensing community to provide the optimal method to reach this goal.

The variation in water levels from the different realizations from the ecotope maps resulted from re-evaluating the ecotope code for each polygon in the ecotope map based on the map purities table from Knotters et al. (2008). The map purity describes the fractional area of the map that is correct for the whole floodplain area, by using a statistical model. In addition, the classification accuracy could well depend on the size of the polygon. For a large polygon, more information is available spatially, spectrally, and contextually, thereby enabling a more informed decision by the manual interpreter. No studies are known that quantify this effect. In this research we assigned new ecotope codes based on the current polygons, thus ignoring the possible effect of polygon size. One way to incorporate this effect would be to overlay the ecotope map with the computational grid from WAQUA, creating may small polygons, and apply the error propagation on this resampled map. As smaller areas will change their ecotope code, the variation of the water level are expected to be more limited than the current findings.

Within-class variation

The variation of vegetation structural characteristics within a single ecotope class can not be parameterized using a hard classification. Even the perfect average per vegetation type can not capture the variability in the field. To assess the effect of spatial differentiation of vegetation structure between polygons of the same vegetation type, a number of realistic combinations of vegetation height and density should be compiled for each vegetation type. These values should be based on a suitable amount of field reference data that is collected specifically for this purpose. These combined values should then be attributed randomly to the polygons subsampled by the WAQUA computational grid. When the variation of the water levels is still unacceptable, vegetation classification alone will not be good enough to parameterize the vegetation roughness. Other remote sensing methods can provide information on the within-class variation, such as airborne laser scanning. Currently,

RWS carries out a pilot to incorporate this within class variation as “ecotope complexes” combinations of existing ecotopes.

Number of runs
In a probabilistic assessment of water levels, the number is runs required to capture the full variation in outcomes is unlimited. Due to computational limitations as suitable number of runs should be determined. In this study, we used twelve runs. The twelfth run gave an extra range of six cm anywhere along the Upper Rhine and Waal section and 13 cm for the IJssel river. This run had a spatial distribution of roughness values that is influenced the water levels more than any of the other realizations. The standard deviation of the differences in water levels did not differ much after ten runs. This indicates the current number of runs was not enough to fully determine the complete range in water levels, and it also suggests that more than 15 runs should not influence the standard deviation much more. Fifteen model runs are therefore suggested for future probabilistic studies. Especially as the size of the ecotopes are to be limited by overlaying with the WAQUA computational grid is expected to limit the effect of classification errors.

Calibration on floodplain roughness
The habitual parameter to calibrate a hydrodynamic model is the roughness of the main channel. This study shows the possible range in values that result from assuming that the floodplain roughness is not correct. In theory, it would be possible to calibrate a flow model on different ecotope distributions as well in a probabilistic manner. Given a discrepancy between model outcome and measured values of water level, or flow velocities, different ecotope distributions can be tested against the measured values. The obvious disadvantage is that no direction for searching can be defined beforehand, making the calibration process more time consuming.

Other uncertainties in the model
The complex system of hydrodynamics that we try to capture in a model has many uncertainties (location, level, and nature). In this study, we quantified the effects of spatial variability of vegetation roughness. Within the ongoing project of uncertain reduction within Flood Control 2015 other aspects are captured, such as morphological changes at the bifurcation points, design discharge and operational discharge prediction. The uncertainties of these other sources should be compared in a final study. One such aspect is the operational work of predicting the water levels during a flood. For this work a 1D model is used, but the sensitivity of this model for roughness parameterization should be studied in more detail.

7. Conclusions and recommendations.

In this study, the sensitivity of a 2D hydrodynamic model was assessed for floodplain roughness parameterisation. Two error sources were studies: (1) classification error, and (2) incorrect values in the lookup table relating ecotopes to vegetation height and density. No absolute errors in water levels result from this approach due to the lack of calibration. We conclude that:

1. The classification error leads to a standard deviation of the water levels per river kilometer of 0.08, 0.05 and 0.10 m for Upper Rhine- Waal, Pannerdensch Kanaal-Nederrijn-Lek and the IJssel river respectively. The range is maximum range in water levels is 0.40, 0.40 and 0.57 m for these river sections respectively. Largest effects are found in the IJssel river and the Pannerdensch Kanaal. The effect of classification accuracy on polygon size is not taken into account in this study.
2. The interquartile range in vegetation height and density in the lookup table leads to a difference in water levels of 0.20, 0.20, and 0.36 m for Upper Rhine- Waal, Pannerdensch Kanaal-Nederrijn-Lek and the IJssel river respectively.
3. The discharge distribution at the Pannerdensche Kop bifurcation point is 165 m^3/s for both errors in classification and lookup table. The discharge distribution at the IJsselkop is more sensitive for classification error than for errors in the lookup table (160 vs. 70 m^3/s for range in classification error and interquartile range in lookup table error).
4. Priority should be given to increasing the classification accuracy as this generates the largest error.
5. The suitable number of runs for a probabilistic assessment of classification accuracy might be fifteen.

Recommendations

- To get a homogeneous size for each of the ecotope polygons the ecotope map can be overlayed with the computational curvilinear grid. In the new realizations the variation would be spatially more varied as the size of individual polygons is smaller. The underlying question that should be answered is whether the size of an individual ecotope polygon influences the quality of classification.
- The changes of water levels due to the variation in discharge distribution is combined with the effect of ecotope roughness variation in this study. It is recommended to investigate separation of these error source in future studies.
- Establish the relation between classification error and variation in water levels.
- Assess the effect of within-class variation of vegetation structure on water levels.
- Determine the effect of other roughness elements such as hedges, single trees, and tree-lined lanes on water levels.

- Check the possibilities to work towards an absolute error assessment of the resulting water levels.
- Assess the effects in an operational 1D model, with respect to flood waves and roughness parameterization in 1D.

References

Amoureus, L. and M. Bomers (2008). Rapport analyse laser data Duursche Waarden (in dutch). Leiderdorp, Fugro Aerial Mapping B.V.**:** 33.

Arcement, G. J. and V. R. Schneider (1989). Guide for selecting Mannings n roughness coefficients for natural channels and floodplains. Reston, Virginia, USA.

Asselman, N. E. M. (2002). Laser altimetry and hydraulic roughness of vegetation, further studies using ground truth. Delft, WL | Delft Hydraulics.

Baptist, M. J., V. Babovich, et al. (2007). "On inducing equations for vegetation resistance." Journal of Hydraulic Research **45**: 435-450.

Baptist, M. J., W. E. Penning, et al. (2004). "Assessment of the effects of cyclic floodplain rejuvenation on flood levels and biodiversity along the Rhine River." River Research and Applications **20**: 285-297.

Bates, P. D., K. J. Marks, et al. (2003). "Optimal use of high-resolution topographic data in flood inundation models." Hydrological Processes **17**(3): 537-557.

Casas, A., G. Benito, et al. (2006). "The topographic data source of digital terrain models as a key element in the accuracy of hydraulic flood modelling." Earth Surface Processes and Landforms **31**(4): 444-456.

Chow, V. T. (1959). Open channel hydraulics. New York, McGraw Hill.

Cobby, D. M., D. C. Mason, et al. (2001). "Image processing of airborne scanning laser altimetry data for improved river flood modeling." ISPRS Journal of Photogrammetry and Remote Sensing **56**: 121-138.

Davenport, I. J., R. B. Bradbury, et al. (2000). "Improving bird population models using airborne remote sensing." International Journal of Remote Sensing **21**(13,14): 2705-2717.

Dawson, F. H. and F. G. Charlton (1988). Bibliography on the hydraulic resistance of vegetated watercourses, Ambleside, Freshwater Biological Association, Occasional Publication.

Geerling, G. W., M. Labrador-Garcia, et al. (2007). "Classification of floodplain vegetation by data-fusion of Spectral (CASI) and LiDAR data." International Journal of Remote Sensing **28**: 4263 – 4284.

Hartman, M. R. and W. E. W. Van den Braak (2007). Baseline manual, baseline 4.03. Arnhem, RIZA**:** 128.

Hopkinson, C., K. Lim, et al. (2004). Wetland grass to plantation forest - estimating vegetation height from the standard deviation of lidar frequency distributions. Laser-scanners for forest and landscape assessment, Freiburg, Germany, Institute for forest growth, Freiburg, Germany.

Houkes, G.H.M, Willems, D. Knotters, and A.G. (2008). Tweede cyclus Rijkswaterstaat ecotopenkartering; biologische monitoring zoete en brakke Rijkswateren. Rijkswaterstaat DID, Delft.

Huthoff, F. and D. Augustijn (2004). Sensitivity analysis of floodplain roughness in 1D flow. 6th Interational conference on hydroinformatics, Singapore, Malaysia.

Jansen, B. J. M. and J. J. G. M. Backx (1998). Ecotope mapping Rhine Branches-east 1997 (in Dutch). Lelystad, RIZA**:** 41.

Järvelä, J. (2004). "Effect of submerged flexible vegetation on flow structure and resistance." Journal of hydrology **307**(1-4): 233-241.

Jesse, P. (2004). Hydraulic resistance in (nature) development (in Dutch). Arnhem, RIZA**:** 65.

Klopstra, D., H. Barneveld, et al. (1997). Analytical model for hydraulic roughness of submerged vegetation. 27th international IAHR conference San Francisco.

Knotters, M. and D. J. Brus (Subm.). "Sampling for validation of ecotope maps of floodplains in the Netherlands." to be checked.

Knotters, M., D. J. Brus, et al. (2008). Validatie van de ecotopenkaarten van de rijkswateren. Wageningen, Alterra**:** 47.

Kouwen, N. (1988). "Field estimation of biomechanical properties of grass." Journal of hydraulic research **26**(5): 559-568.

Kouwen, N. (2000). "Friction factors for coniferous trees along rivers." Journal of hydraulic engineering **126**(10): 732-740.

Kouwen, N. and R. M. Li (1980). "Biomechanics of vegetated channel linings." Journal of Hydraulics Divisions **106**(6): 1085-1103.

Kouwen, N., T. E. Unny, et al. (1969). "Flow retardance in vegetated channels." Journal of the Irrigation and Drainage Division **95(IR2)**: 329-342.

Mertes, L. A. K. (2002). "Remote sensing of riverine landscapes." Freshwater Biology **47**: 799-816.

Petryk, S. and G. Bosmajian (1975). "Analysis of flow through vegetation." Journal of hydraulics divisions **101**: 871-884.

Postma, L., G. K. Verboom, et al. (2000). Towards an Open Delft3D Modelling System. Hydroinformatics 2000, Iowa, Iowa Institute of Hydrological Research.

Ringrose, S., W. Matheson, et al. (1988). "Differentiation of ecological zones in the Okavango delta, Botswana by classification and contextual analyses of Landsat MSS data." Photogrammetric Engineering & Remote Sensing **54**(5): 601-608.

RWS. (2007). "Users guide WAQUA: Technical Report SIMONA 92-10." Retrieved 13-02-2008, from http://www.waqua.nl/systeem/documentatie/usedoc/slib3d/ug-slib3d.pdf,.

RWS. (2008). “Voorlopig rivierkundig beoordelingskader voor ingrepen in de Rijntakken” RWS-Oost Nederland, PKB-RvdR, RWS-RIZA, werkdocument.

Schmidt, K. S. and A. K. Skidmore (2003). "Spectral discrimination of vegetation types in a coastal wetland." Remote Sensing of Environment **85**(1): 92-108.

Stolker, C., E. H. Van Velzen, et al. (1999). Nauwkeurigheidsanalyse stromingsweerstand vegetatie (in Dutch). Delft, Arnhem, Delft Hydraulics, RIZA**:** 21.

Straatsma, M. W. (2008). "Quantitative mapping of hydrodynamic vegetation density of floodplain forests using airborne laser scanning." Photogrammetric Engineering and Remote Sensing **47**(8): 987-998.

Straatsma, M. W. (2009). "3D float tracking: <I>in situ</I> floodplain roughness estimation." Hydrological Processes **23**(2): 201-212.

Straatsma, M. W. and M. J. Baptist (2008). "Floodplain roughness parameterization using airborne laser scanning and spectral remote sensing." Remote Sensing of Environment **112**(3): 1062-1080.

Straatsma, M. W. and H. Middelkoop (2007). "Extracting structural characteristics of herbaceous floodplain vegetation for hydrodynamic modeling using airborne laser scanner data." International Journal of Remote Sensing **28**: 2447-2467.

Straatsma, M. W. and M. R. Ritzen (2002). Laseraltimetrie en vegetatieruwheid van uiterwaarden (in Dutch). Physical Geography. Utrecht, Utrecht University. **MSc:** 117.

Straatsma, M. W., J. J. Warmink, et al. (2008). "Two novel methods for field measurements of hydrodynamic density of floodplain vegetation using terrestrial laser scanning and digital parallel photography." International Journal of Remote Sensing **29**(5): 1595-1617.

Townsend, P. A. and J. Walsh (2001). "Remote sensing of forested wetlands: application of multitemporal and multispectral satellite imagery to determine plant community composition and structure in southeastern USA." Plant Ecology **157**: 129-149.

Van der Klis, H. (2003). Uncertainty analysis applied to numerical models of river bed morphology. Delft, Delft University of Technology. **PhD**.

Van der Klis, H., S. Van Vuren, et al. (2006). Zicht op onzekerheden in de PKB Ruimte voor de rivier. Delft, WL|Delft Hydraulics.

Van der Molen, D. T., N. Geilen, et al. (2003). "Water Ecotope Classification for integrated water management in the Netherlands. European Water Management Online." 2003, from http://www.ewaonline.de/journal/2003_03.pdf.

Van der Sande, C. J., S. M. De Jong, et al. (2003). "A segmentation and classification approach of IKONOS-2 imagery for land cover mapping to assist flood risk and flood damage assessment." International Journal of Applied Earth Observation and Geoinformation **4**: 217-229.

Van Rijn, L. C. (1994). Principles of fluid flow and surface waves in rivers, estuaries, seas and oceans. Amsterdam, Aqua publications.

Van Stokkom, H. T. C., A. J. M. Smits, et al. (2005). "Flood defense in the Netherlands a new era, a new approach." Water International **30**(1): 76-87.

Van Velzen, E. H., P. Jesse, et al. (2003). Stromingsweerstand vegetatie in uiterwaarden (in Dutch). Arnhem, RIZA**:** 131.

Van Vuren, S. (2005). Stochastic modeling of river morphodynamics. Civil Engineering. Delft, Delft University of Technology. **PhD**.

Walker, W. E., P. Harremoes, et al. (2003). "Defining Uncertainty A Conceptual Basis for Uncertainty Management in Model-Based Decision Support." Integrated Assessment **4**(1): 5-17.

Warmink, J. (2007). Vegetation density measurements using parallel photography and terrestrial laser scanning. Department of Physical Geography. Utrecht, Utrecht University. **MSc:** 80.

Appendix A 1: Names of the ecotopes and associated Baseline 4 roughness codes

Ecotope code	Description	Roughness code baseline 4	Roughness code description
HA-1	Highwater free agriculture	121	Agricultural land
HA-2	Highwater free builtup area	114	Paved / Builtup area
HB-1	Highwater free natural forest	1244	Natural forest
HB-2	Highwater free shrubs	1233	Shrubs
HB-3	Highwater free production forest	1242	Production forest
HG-1	Highwater free natural grassland	1202	Natural meadows
HG-1-2	Highwater free grassland (natural or production)	1202	Production / natural meadows
HG-2	Highwater free production grassland	1201	Production meadows
HM-1	Highwater free reeds	1807	Reeds and other helophytes
HR-1	Highwater free herbaceous vegetation	1212	Herbaceous vegetation
H-REST	Highwater free temporarily bare	1250	Rest
I.1	Dynamic sweet to brackish shallow water	106	Shallow water
I.3	Slightly dynamic sweet to brackish shallow water	106	Shallow water
II.1	Gravel bars	111	Bare river bar
II.2	Sweet sand bars	111	Bare river bar
II.2-3	Sweet sand bars/ sweet mud banks	111	Bare river bar
II.3	Sweet mud banks	111	Bare river bar
II.4-5	Mid to highly dynamic brackish and salty bars	111	Bare river bar
III.2	Highly dynamic hard substrate influenced by sweet to brackish water	113	Paved / Builtup area
III.2-3	Low dynamic hard substrate influenced by sweet to brackish water	113	Paved / Builtup area
III.4	Low dynamic hard substrate influenced by brackish water	113	Paved / Builtup area
III.8	Low dynamic hard substrate on the outside berm influenced by salty water	113	Paved / Builtup area
IV.1	Species poor helophytes in shallow sweet water	1807	Reeds and other helophytes
IV.3-IV.8	Species poor helophytes swamp	1224	Bulrush / other helophytes
IV.7	Brackish helophyte culture	1807	Reeds and other helophytes
IV.8-9	Species poor helophytes swamp/Species rich reed swamp	1807	Reeds and other helophytes
IX.a	Agriculture on the shoreline	121	Agricultural land
OK-1	Unvegetated natural levee	1250	Bare levee
O-UA-1	Natural levee or floodplain agriculture	121	Agricultural land
O-UA-2	Natural levee or floodplain builtup area	114	Paved / Builtup area
O-UB-1	Natural levee or floodplain forest	1245	Natural forest
O-UB-2	Natural levee or floodplain shrubs	1231	Shrubs
O-UB-3	Natural levee or floodplain production forest	1242	Production forest
O-UG-1	Natural levee or floodplain grass land	1202	Natural grassland
O-UG-1-2	Natural levee or floodplain grass land (natural or production)	1202	Production / natural meadows
O-UG-2	Natural levee or floodplain production grassland	1201	Production meadows
O-UK-1	Natural levee or floodplain unvegetated	1250	Bare levee
O-UR-1	Natural levee or floodplain herbaceous vegetation	1212	Herbaceous vegetation
O-U-REST	Natural levee or floodplain temporarily bare	1250	Rest
R	Temporarily bare	1250	Rest
REST	Temporarily bare	1250	Rest
REST-O	Temporarily bare	1250	Rest
REST-O-T	Temporarily bare	1250	Rest
REST-T	Temporarily bare high water free	1250	Rest
RnM	Moderately deep side channel	105	Side channel
RnMz-h	Moderately deep side channel	105	Side channel
RnOz-h	Moderately deep side channel	105	Side channel
RvD	(Very) deep	106	River accompanying water
RvDz-k-h	(Very) deep	106	River accompanying water
RvDz-k-h/RvMz-k-h	(Very) deep / moderately deep	106	River accompanying water
RvM	Moderately deep water	106	River accompanying water
RvMz-k-h	Moderately deep water	106	River accompanying water
RvO	Shallow water	106	River accompanying water
RvOz-k-h	Shallow water	106	River accompanying water
RwD	(Very) deep water	106	River accompanying water
RwM	Moderately deep water	106	River accompanying water
RwMz-h	Moderately deep water	106	River accompanying water
RwO	Shallow water	106	River accompanying water

Appendix A 2: Names of the ecotopes and associated Baseline 4 roughness codes

Ecotope code	Description	Roughness code baseline 4	Roughness code description
RwOz-h	Shallow water	106	River accompanying water
RzD	Deep main channel	102	Main channel
RzDz-h	Deep main channel	102	Main channel
RzM	Moderately deep main channel	102	Main channel
RzMz-h	Moderately deep main channel	102	Main channel
RzO	Shallow main channel	102	Main channel
RzOz-h	Shallow main channel	102	Main channel
UA-1	Floodplain agriculture	121	Agricultural land
UA-2	Floodplain builtup area	114	Paved / Builtup area
UB-1	Floodplain forest	1245	Natural forest
UB-2	Floodplain shrubs	1231	Shrubs
UB-3	Floodplain production forest	1242	Production forest
UG-1	Floodplain grass land	1202	Natural grassland
UG-1-2	Floodplain grass land (natural or production)	1202	Production / natural meadows
UG-2	Floodplain production grass land	1201	Production meadows
UG-HA-2	Floodplain production grass land / Highwater free production grass land	114	Production meadow / builtup
U-HG-2	Floodplain production grass land / Highwater free builtup area	1201	Production meadow
UM-1	Natural levee or floodplain reed	1807	Reeds and other helophytes
UR-1	Floodplain herbaceous vegetation	1212	Herbaceous vegetation
U-REST	Floodplain temporarily bare	1250	Rest
V.1-2	Floodplain swamp	1804	Herbaceous vegetation
V.2	Species poor reed swamp	1804	Reeds and other helophytes
V.2/UR-1-2	Species poor reed swamp/floodplain natural grass land/floodplain production grass land	1202	Herbaceous vegetation
V.4/UR-1	Species poor, stucture rich floodplain herbaceous vegetation	1212	Herbaceous vegetation
VI.2	Softwood shrubs	1231	Shrubs
VI.2-3	Softwood shrubs or pioneer softwood forest	1231	Shrubs
VI.4	Softwood forest	1245	Natural forest
VI.5	Floodplain forest	1242	Natural forest
VI.7	Floodplain willow production forest	1232	Willow production forest
VI.8	Production forest on shoreline	1242	Production forest
VI.g	Production / natural grass land	1202	Production / natural meadows
VI.nb	Natural forest	1245	Natural forest
VI.pb	Production forest	1242	Production forest
VII.1	Swampy inundation grass land	1202	Natural grassland
VII.1-2	Swampy inundation grass land / structure rich grass land	1202	Natural grassland
VII.1-2-3	Swampy inundation grass land / structure rich grass land/ production grass land	1202	Production / natural meadows
VII.1-3	Swampy inundation grass land / structure rich grass land/ production grass land	1202	Production / natural meadows
VII.2	Structure rich grass land	1202	Natural meadows
VII.3	Production grass land	1201	Production meadow

Appendix B 1. Map purities given by Knotters et al. (2008)

	FIELD													
MAP	HA-1	HA-2	HB-1	HB-2	HB-3	HG-1	HG-1-2	HG-2	HK-1	HK-2	HR-1	II.2	IV.1-2	IV.8-9
H-REST	0	0.486	0	0.353	0	0	0	0	0.162	0	0	0	0	0
HA-1	0	0	0	0	0	0	0	0.086	0	0	0	0	0	0
HA-2	0	0.842	0	0	0.018	0	0	0.018	0	0	0	0	0	0
HB-1	0	0.298	0.318	0	0.06	0	0	0	0	0	0	0	0	0
HB-2	0	0.092	0.105	0.214	0.02	0.054	0	0	0	0	0.054	0	0	0
HB-3	0	0.138	0	0.18	0.222	0	0	0	0	0	0	0	0	0
HG-1	0	0	0	0	0	0.173	0	0.198	0	0	0	0	0	0
HG-1-2	0	0	0	0	0	0	0	0.496	0	0	0	0	0	0.257
HG-2	0.009	0	0	0	0.052	0	0.078	0.193	0	0	0	0	0	0
HM-1	0	0	0	0	0	0	0	0	0	0	0	0	0	0
HR-1	0	0	0	0.079	0	0.093	0	0.079	0	0	0.289	0	0	0.101
II.2	0	0	0	0	0	0	0	0	0	0	0	0.858	0	0
III.2-3	0	0.2	0	0	0	0	0	0	0	0	0	0	0	0
IV.8-9	0	0	0	0	0	0	0	0	0	0	0	0	0.332	0.503
IX.a	0	0	0	0	0	0	0	0	0	0	0	0	0	0
O-UA-2	0	0	0	0	0	0	0	0	0	0	0	0	0	0
O-UB-1	0	0	0	0	0	0	0	0	0	0	0	0	0	0
O-UG-1	0	0	0	0	0	0	0	0	0	0	0	0	0	0
O-UG-1-2	0	0	0	0	0	0	0	0	0	0	0	0	0	0
O-UG-2	0	0	0	0	0	0	0	0	0	0	0	0	0	0
O-UR-1	0	0	0	0	0	0	0	0	0	0	0	0	0	0
OK-1	0	0	0	0	0	0	0	0	0	0	0	0	0	0
REST	0	0	0	0	0	0	0	0	0	0	0	0.685	0	0
U-REST	0	1	0	0	0	0	0	0	0	0	0	0	0	0
UA-1	0.108	0	0	0	0	0	0	0	0	0	0	0	0	0
UA-2	0	0.486	0	0	0	0	0	0	0	0	0	0	0	0
UB-1	0	0	0	0.068	0	0	0	0	0	0	0	0	0	0
UB-2	0	0	0	0.274	0.117	0	0	0	0	0	0.117	0	0	0
UB-3	0	0	0	0	0.135	0	0	0	0	0	0	0	0	0
UG-1	0	0	0	0	0	0.042	0	0.042	0	0	0	0	0	0
UG-1-2	0	0	0	0	0.039	0	0	0.128	0	0	0.089	0	0	0
UG-2	0	0	0	0	0	0	0	0	0	0	0	0	0	0
UM-1	0	0	0	0	0	0	0	0	0	0	0	0	0	0.448
UR-1	0	0	0	0	0	0	0	0	0	0.094	0	0	0	0
V.1-2	0	0	0	0	0	0	0	0	0	0	0	0	0	0
VI.2-3	0	0	0	0	0	0	0	0.06	0	0	0	0	0.071	0
VI.4	0	0	0	0	0	0	0	0	0.087	0	0	0	0	0
VI.7	0	0	0	0	0	0	0	0	0	0	0	0	0	0
VI.8	0	0	0	0	0.222	0	0	0	0	0	0	0	0	0
VII.1	0	0	0	0	0	0	0	0	0	0	0	0	0	0
VII.1-3	0	0	0	0	0	0	0	0.137	0	0	0	0	0	0
VII.3	0	0	0	0	0	0	0	0	0	0	0	0.321	0	0

Appendix B 2. Map purities given by Knotters et al. (2008)

	FIELD													
MAP	O-UG-1	OA-2	OB-1	OB-2	OB-4	OG-1	OG-2	OK-1	OR-1	UA-1	UA-2	UB-1	UB-2	UB-3
H-REST	0	0	0	0	0	0	0	0	0	0	0	0	0	0
HA-1	0	0	0	0	0	0	0	0	0	0.783	0	0	0	0
HA-2	0	0.055	0	0.018	0	0	0	0	0	0	0.049	0	0	0
HB-1	0	0	0	0.062	0.055	0	0	0	0	0	0	0.097	0	0.055
HB-2	0	0	0	0.02	0.059	0	0	0	0	0	0	0	0.117	0
HB-3	0	0	0	0	0	0	0	0	0	0	0.138	0.161	0	0
HG-1	0	0.087	0	0	0	0.129	0.099	0	0	0	0	0	0	0
HG-1-2	0	0	0	0	0	0	0	0	0	0	0	0	0	0
HG-2	0	0	0	0	0.026	0.074	0.136	0	0	0.024	0	0.009	0	0
HM-1	0	0	0	0	0	0	0	0	0	0	0	0	0	0
HR-1	0	0	0	0	0	0	0	0	0.035	0.093	0	0	0	0
II.2	0	0	0	0	0	0	0	0	0	0	0	0	0	0
III.2-3	0	0.599	0	0.2	0	0	0	0	0	0	0	0	0	0
IV.8-9	0	0	0	0	0	0	0	0	0	0	0	0	0	0
IX.a	0	0	0	0	0	0	0	0	0	1	0	0	0	0
O-UA-2	0	0	0	0	0	0	0	0	0	0	0	0	0	0
O-UB-1	0	0	0.331	0	0	0	0	0	0.331	0	0	0	0	0
O-UG-1	0.247	0	0	0	0	0.538	0.108	0	0	0	0	0	0	0
O-UG-1-2	0	0	0	0	0	0	0.685	0.315	0	0	0	0	0	0
O-UG-2	0	0	0	0	0	0.336	0.328	0	0	0	0	0	0	0
O-UR-1	0	0	0	0	0	0.145	0	0.145	0.145	0	0	0	0	0.145
OK-1	0	0	0	0	0	0.786	0	0.214	0	0	0	0	0	0
REST	0	0	0	0	0	0	0	0	0	0	0.315	0	0	0
U-REST	0	0	0	0	0	0	0	0	0	0	0	0	0	0
UA-1	0	0	0	0	0	0	0.092	0	0	0.616	0	0	0	0
UA-2	0	0.271	0	0	0	0	0	0	0	0	0	0	0	0
UB-1	0	0	0.08	0	0	0	0	0	0	0	0	0.675	0.068	0
UB-2	0	0	0	0	0	0	0	0	0	0	0	0	0.239	0.117
UB-3	0	0	0	0	0	0	0	0	0	0	0	0.315	0	0.392
UG-1	0	0	0	0	0	0.322	0	0	0	0	0	0	0	0
UG-1-2	0	0	0	0	0	0.208	0	0	0	0	0	0	0	0
UG-2	0	0	0	0	0	0.062	0.127	0	0	0	0	0	0	0
UM-1	0	0	0	0	0	0	0	0	0	0	0	0	0	0
UR-1	0	0	0	0	0	0	0	0	0.07	0	0	0	0	0
V.1-2	0	0	0	0	0	0.14	0	0	0.36	0	0	0.03	0	0
VI.2-3	0	0	0	0.079	0.077	0	0	0	0	0	0	0	0.026	0
VI.4	0	0	0.267	0.065	0	0	0	0	0	0	0	0.356	0	0
VI.7	0	0	1	0	0	0	0	0	0	0	0	0	0	0
VI.8	0	0	0.519	0	0	0	0	0	0	0	0	0	0	0.259
VII.1	0	0	0	0	0	0.189	0	0	0	0	0	0	0	0
VII.1-3	0	0	0	0	0	0	0	0	0.183	0	0	0	0	0
VII.3	0	0	0	0	0	0.321	0	0	0	0	0	0	0	0

Appendix B 3. Map purities given by Knotters et al. (2008)

	FIELD												
MAP	UG-1	UG-2	UR-1	UR-1-2	V.1-2	VI.1	VI.1-2	VI.2	VI.2-3	VI.4	VI.7	VII.1	VII.2
H-REST	0	0	0	0	0	0	0	0	0	0	0	0	0
HA-1	0	0.131	0	0	0	0	0	0	0	0	0	0	0
HA-2	0	0	0	0	0	0	0	0	0	0	0	0	0
HB-1	0	0	0	0	0	0	0	0	0	0.055	0	0	0
HB-2	0	0	0.046	0.059	0	0	0	0	0	0.161	0	0	0
HB-3	0	0	0	0	0	0	0	0	0	0.161	0	0	0
HG-1	0.116	0.198	0	0	0	0	0	0	0	0	0	0	0
HG-1-2	0.118	0	0	0	0.129	0	0	0	0	0	0	0	0
HG-2	0.084	0.288	0	0.027	0	0	0	0	0	0	0	0	0
HM-1	0	0	0	0	1	0	0	0	0	0	0	0	0
HR-1	0.093	0	0	0.138	0	0	0	0	0	0	0	0	0
II.2	0	0	0	0	0	0	0.071	0	0.071	0	0	0	0
III.2-3	0	0	0	0	0	0	0	0	0	0	0	0	0
IV.8-9	0	0	0	0	0	0	0	0	0.166	0	0	0	0
IX.a	0	0	0	0	0	0	0	0	0	0	0	0	0
O-UA-2	0	1	0	0	0	0	0	0	0	0	0	0	0
O-UB-1	0	0	0	0	0	0	0	0	0.339	0	0	0	0
O-UG-1	0.108	0	0	0	0	0	0	0	0	0	0	0	0
O-UG-1-2	0	0	0	0	0	0	0	0	0	0	0	0	0
O-UG-2	0	0	0	0.336	0	0	0	0	0	0	0	0	0
O-UR-1	0	0	0	0	0	0	0	0	0.422	0	0	0	0
OK-1	0	0	0	0	0	0	0	0	0	0	0	0	0
REST	0	0	0	0	0	0	0	0	0	0	0	0	0
U-REST	0	0	0	0	0	0	0	0	0	0	0	0	0
UA-1	0	0.184	0	0	0	0	0	0	0	0	0	0	0
UA-2	0	0.243	0	0	0	0	0	0	0	0	0	0	0
UB-1	0	0	0	0	0	0	0	0	0.03	0.08	0	0	0
UB-2	0	0	0	0	0	0.137	0	0	0	0	0	0	0
UB-3	0	0.158	0	0	0	0	0	0	0	0	0	0	0
UG-1	0.21	0.096	0.192	0	0	0	0	0	0	0	0	0.096	0
UG-1-2	0.255	0.282	0	0	0	0	0	0	0	0	0	0	0
UG-2	0.322	0.325	0	0.085	0	0	0	0.042	0	0	0	0.036	0
UM-1	0	0	0	0	0.552	0	0	0	0	0	0	0	0
UR-1	0.035	0	0.08	0.547	0.08	0	0	0	0	0	0.094	0	0
V.1-2	0.08	0	0	0.229	0	0.08	0	0	0.08	0	0	0	0
VI.2-3	0	0	0	0.097	0	0.105	0	0	0.246	0.168	0	0	0.071
VI.4	0	0	0	0	0	0	0	0	0.032	0.193	0	0	0
VI.7	0	0	0	0	0	0	0	0	0	0	0	0	0
VI.8	0	0	0	0	0	0	0	0	0	0	0	0	0
VII.1	0.378	0	0	0	0	0	0	0	0	0	0	0.433	0
VII.1-3	0	0	0	0	0	0	0	0	0	0	0	0.496	0.183
VII.3	0.358	0	0	0	0	0	0	0	0	0	0	0	0

Appendix C 1: Adjusted error matrix

ECOCODE	H-REST	HA-1	HA-2	HB-1	HB-2	HB-3	HG-1	HG-1-2	HG-2	HM-1	HR-1	I.1	II.2	III.2-3
H-REST	0.162	0	0.486	0	0.353	0	0	0	0	0	0	0	0	0
HA-1	0	0	0	0	0	0	0	0	0.071	0	0	0	0	0
HA-2	0	0	0.842	0	0	0.018	0	0	0.018	0	0	0	0	0
HB-1	0	0	0.298	0.318	0	0.06	0	0	0	0	0	0	0	0
HB-2	0	0	0.092	0.105	0.214	0.02	0.054	0	0	0	0.054	0	0	0
HB-3	0	0	0.138	0	0.18	0.222	0	0	0	0	0	0	0	0
HG-1	0	0	0	0	0	0	0.15	0	0.172	0	0	0	0	0
HG-1-2	0	0	0	0	0	0	0	0	0.496	0	0	0	0	0
HG-2	0	0.009	0	0	0	0.052	0	0.078	0.193	0	0	0	0	0
HM-1	0	0	0	0	0	0	0	0	0	0	0	0	0	0
HR-1	0	0	0	0	0.079	0	0.093	0	0.079	0	0.289	0	0	0
I.1	0	0	0	0	0	0	0	0	0	0	0	1	0	0
II.2	0	0	0	0	0	0	0	0	0	0	0	0	0.858	0
III.2-3	0	0	0.2	0	0	0	0	0	0	0	0	0	0	0
IV.8-9	0	0	0	0	0	0	0	0	0	0	0	0	0	0
IX.a	0	0	0	0	0	0	0	0	0	0	0	0	0	0
O-U-REST	0.2	0	0	0	0	0	0	0	0	0	0	0	0	0
O-UA-1	0	0	0	0	0	0	0.05	0.05	0	0	0	0	0	0
O-UA-2	0	0	0	0	0	0	0	0	0	0	0	0	0	0
O-UB-1	0	0	0	0	0	0	0	0	0	0	0	0	0	0
O-UB-2	0	0	0	0.098	0	0	0	0	0	0	0	0	0	0
O-UB-3	0	0	0	0	0	0.15	0	0	0	0	0	0	0	0
O-UG-1	0	0	0	0	0	0	0	0	0	0	0	0	0	0
O-UG-1-2	0	0	0	0	0	0	0	0	0	0	0	0	0	0
O-UG-2	0	0	0	0	0	0	0	0	0	0	0	0	0	0
O-UK-1	0	0	0	0	0	0	0	0.1	0	0	0	0	0	0
O-UR-1	0	0	0	0	0	0	0	0	0	0	0	0	0	0
OK-1	0	0	0	0	0	0	0	0	0	0	0	0	0	0
R	0	0	0	0	0	0	0	0	0	0	0	0	0.35	0
REST	0	0	0	0	0	0	0	0	0	0	0	0	0.685	0
RnM	0	0	0	0	0	0	0	0	0	0	0	0	0	0
RvD	0	0	0	0	0	0	0	0	0	0	0	0	0	0
RvM	0	0	0	0	0	0	0	0	0	0	0	0	0	0
RvO	0	0	0	0	0	0	0	0	0	0	0	0	0	0
RwD	0	0	0	0	0	0	0	0	0	0	0	0	0	0
RwM	0	0	0	0	0	0	0	0	0	0	0	0	0	0
RwO	0	0	0	0	0	0	0	0	0	0	0	0	0	0
RzD	0	0	0	0	0	0	0	0	0	0	0	0	0	0
RzM	0	0	0	0	0	0	0	0	0	0	0	0	0	0
RzO	0	0	0	0	0	0	0	0	0	0	0	0	0	0
U-REST	0	0	1	0	0	0	0	0	0	0	0	0	0	0
UA-1	0	0.108	0	0	0	0	0	0	0	0	0	0	0	0
UA-2	0	0	0.486	0	0	0	0	0	0	0	0	0	0	0
UB-1	0	0	0	0	0.068	0	0	0	0	0	0	0	0	0
UB-2	0	0	0	0	0.245	0.105	0	0	0	0	0.105	0	0	0
UB-3	0	0	0	0	0	0.119	0	0	0	0	0	0	0	0
UG-1	0	0	0	0	0	0	0.042	0	0.042	0	0	0	0	0
UG-1-2	0	0	0	0	0	0.037	0	0	0.123	0	0.085	0	0	0
UG-2	0	0	0	0	0	0	0	0	0	0	0	0	0	0
UM-1	0	0	0	0	0	0	0	0	0	0	0	0	0	0
UR-1	0.094	0	0	0	0	0	0	0	0	0	0	0	0	0
V.1-2	0	0	0	0	0	0	0	0	0	0	0	0	0	0
VI.2-3	0	0	0	0	0	0	0	0	0.06	0	0	0	0	0
VI.4	0.087	0	0	0	0	0	0	0	0	0	0	0	0	0
VI.7	0	0	0	0	0	0	0	0	0	0	0	0	0	0
VI.8	0	0	0	0	0	0.181	0	0	0	0	0	0	0	0
VII.1	0	0	0	0	0	0	0	0	0	0	0	0	0	0
VII.1-3	0	0	0	0	0	0	0	0	0.137	0	0	0	0	0
VII.3	0	0	0	0	0	0	0	0	0	0	0	0	0.321	0

Appendix C 2: Adjusted error matrix

ECOCODE	IV.8-9	IX.a	O-U-REST	O-UA-1	O-UA-2	O-UB-1	O-UB-2	O-UG-1	O-UG-1-2	O-UG-2	O-UK-1	O-UR-1	OK-1	R
H-REST	0	0	0	0	0	0	0	0	0	0	0	0	0	0
HA-1	0	0	0	0.167	0	0	0	0	0	0	0	0	0	0
HA-2	0	0	0	0	0.055	0	0.018	0	0	0	0	0	0	0
HB-1	0	0	0	0	0	0	0.117	0	0	0	0	0	0	0
HB-2	0	0	0	0	0	0	0.079	0	0	0	0	0	0	0
HB-3	0	0	0	0	0	0	0	0	0	0	0	0	0	0
HG-1	0	0	0	0.13	0.075	0	0	0.113	0	0.086	0	0	0	0
HG-1-2	0.257	0	0	0	0	0	0	0	0	0	0	0	0	0
HG-2	0	0	0	0	0	0	0.026	0.074	0	0.136	0	0	0	0
HM-1	0	0	0	0	0	0	0	0	0	0	0	0	0	0
HR-1	0.101	0	0	0	0	0	0	0	0	0	0	0.035	0	0
I.1	0	0	0	0	0	0	0	0	0	0	0	0	0	0
II.2	0	0	0	0	0	0	0	0	0	0	0	0	0	0
III.2-3	0	0	0	0	0.599	0	0.2	0	0	0	0	0	0	0
IV.8-9	0.834	0	0	0	0	0	0	0	0	0	0	0	0	0
IX.a	0	0	0	0	0	0	0	0	0	0	0	0	0	0
O-U-REST	0	0	0.3	0.1	0	0	0	0	0	0	0	0	0.1	0
O-UA-1	0	0	0.1	0.6	0	0	0	0.05	0.05	0.1	0	0	0	0
O-UA-2	0	0	0	0	0	0	0	0	0	0	0	0	0	0
O-UB-1	0	0	0	0	0	0.312	0	0	0	0	0	0.312	0	0
O-UB-2	0	0	0	0	0	0.098	0.49	0	0	0	0	0	0	0
O-UB-3	0	0	0	0	0.1	0.07	0.08	0	0	0	0	0	0	0
O-UG-1	0	0	0	0.231	0	0	0	0.603	0	0.083	0	0	0	0
O-UG-1-2	0	0	0	0.071	0	0	0	0	0	0.49	0.214	0	0.225	0
O-UG-2	0	0	0	0.087	0	0	0	0.292	0	0.285	0	0	0	0
O-UK-1	0	0	0	0	0	0	0	0.3	0.3	0	0.25	0	0	0
O-UR-1	0	0	0	0	0	0	0	0.126	0	0	0.13	0.126	0.126	0
OK-1	0	0	0	0	0	0	0	0.655	0	0	0.167	0	0.178	0
R	0	0	0	0	0.05	0	0.1	0	0	0	0	0	0	0.5
REST	0	0	0	0	0	0	0	0	0	0	0	0	0	0
RnM	0	0	0	0	0	0	0	0	0	0	0	0	0	0
RvD	0	0	0	0	0	0	0	0	0	0	0	0	0	0
RvM	0	0	0	0	0	0	0	0	0	0	0	0	0	0
RvO	0	0	0	0	0	0	0	0	0	0	0	0	0	0
RwD	0	0	0	0	0	0	0	0	0	0	0	0	0	0
RwM	0	0	0	0	0	0	0	0	0	0	0	0	0	0
RwO	0	0	0	0	0	0	0	0	0	0	0	0	0	0
RzD	0	0	0	0	0	0	0	0	0	0	0	0	0	0
RzM	0	0	0	0	0	0	0	0	0	0	0	0	0	0
RzO	0	0	0	0	0	0	0	0	0	0	0	0	0	0
U-REST	0	0	0	0	0	0	0	0	0	0	0	0	0	0
UA-1	0	0	0	0	0	0	0	0	0	0.092	0	0	0	0
UA-2	0	0	0	0	0.271	0	0	0	0	0	0	0	0	0
UB-1	0	0	0	0	0	0.08	0	0	0	0	0	0	0	0
UB-2	0	0	0	0	0	0	0	0	0	0	0	0	0	0
UB-3	0	0	0	0	0	0	0	0	0	0	0	0	0	0
UG-1	0	0	0	0	0	0	0	0.322	0	0	0	0	0	0
UG-1-2	0	0	0	0	0	0	0	0.2	0	0	0	0	0	0
UG-2	0	0	0	0	0	0	0	0.062	0	0.127	0	0	0	0
UM-1	0.448	0	0	0	0	0	0	0	0	0	0	0	0	0
UR-1	0	0	0	0	0	0	0	0	0	0	0	0.07	0	0
V.1-2	0	0	0	0	0	0	0	0.14	0	0	0	0.36	0	0
VI.2-3	0.071	0	0	0	0	0	0.156	0	0	0	0	0	0	0
VI.4	0	0	0	0	0	0.267	0.065	0	0	0	0	0	0	0
VI.7	0	0	0	0	0	1	0	0	0	0	0	0	0	0
VI.8	0	0	0	0	0	0.425	0	0	0	0	0	0	0	0
VII.1	0	0	0	0	0	0	0	0.189	0	0	0	0	0	0
VII.1-3	0	0	0	0	0	0	0	0	0	0	0	0.183	0	0
VII.3	0	0	0	0	0	0	0	0.321	0	0	0	0	0	0

Appendix C 3: Adjusted error matrix

ECOCODE	REST	RnM	RvD	RvM	RvO	RwD	RwM	RwO	RzD	RzM	U-REST	UA-1	UA-2	UB-1
H-REST	0	0	0	0	0	0	0	0	0	0	0	0	0	0
HA-1	0	0	0	0	0	0	0	0	0	0	0	0.653	0	0
HA-2	0	0	0	0	0	0	0	0	0	0	0	0	0.049	0
HB-1	0	0	0	0	0	0	0	0	0	0	0	0	0	0.097
HB-2	0	0	0	0	0	0	0	0	0	0	0	0	0	0
HB-3	0	0	0	0	0	0	0	0	0	0	0	0	0.138	0.161
HG-1	0	0	0	0	0	0	0	0	0	0	0	0	0	0
HG-1-2	0	0	0	0	0	0	0	0	0	0	0	0	0	0
HG-2	0	0	0	0	0	0	0	0	0	0	0	0.024	0	0.009
HM-1	0	0	0	0	0	0	0	0	0	0	0	0	0	0
HR-1	0	0	0	0	0	0	0	0	0	0	0	0.093	0	0
I.1	0	0	0	0	0	0	0	0	0	0	0	0	0	0
II.2	0	0	0	0	0	0	0	0	0	0	0	0	0	0
III.2-3	0	0	0	0	0	0	0	0	0	0	0	0	0	0
IV.8-9	0	0	0	0	0	0	0	0	0	0	0	0	0	0
IX.a	0	0	0	0	0	0	0	0	0	0	0	1	0	0
O-U-REST	0	0	0	0	0	0	0	0	0	0	0.2	0.1	0	0
O-UA-1	0	0	0	0	0	0	0	0	0	0	0	0	0	0
O-UA-2	0	0	0	0	0	0	0	0	0	0	0	0	0	0
O-UB-1	0	0	0	0	0	0	0	0	0	0	0	0	0	0
O-UB-2	0	0	0	0	0	0	0	0	0	0	0	0	0.049	0
O-UB-3	0	0	0	0	0	0	0	0	0	0	0	0	0	0
O-UG-1	0	0	0	0	0	0	0	0	0	0	0	0	0	0
O-UG-1-2	0	0	0	0	0	0	0	0	0	0	0	0	0	0
O-UG-2	0	0	0	0	0	0	0	0	0	0	0	0	0	0
O-UK-1	0	0	0	0	0	0	0	0	0	0	0	0	0	0
O-UR-1	0	0	0	0	0	0	0	0	0	0	0	0	0	0
OK-1	0	0	0	0	0	0	0	0	0	0	0	0	0	0
R	0	0	0	0	0	0	0	0	0	0	0	0	0	0
REST	0	0	0	0	0	0	0	0	0	0	0	0	0.315	0
RnM	0	1	0	0	0	0	0	0	0	0	0	0	0	0
RvD	0	0	1	0	0	0	0	0	0	0	0	0	0	0
RvM	0	0	0	1	0	0	0	0	0	0	0	0	0	0
RvO	0	0	0	0	1	0	0	0	0	0	0	0	0	0
RwD	0	0	0	0	0	1	0	0	0	0	0	0	0	0
RwM	0	0	0	0	0	0	1	0	0	0	0	0	0	0
RwO	0	0	0	0	0	0	0	1	0	0	0	0	0	0
RzD	0	0	0	0	0	0	0	0	1	0	0	0	0	0
RzM	0	0	0	0	0	0	0	0	0	1	0	0	0	0
RzO	0	0	0	0	0	0	0	0	0	0	0	0	0	0
U-REST	0	0	0	0	0	0	0	0	0	0	0	0	0	0
UA-1	0	0	0	0	0	0	0	0	0	0	0	0.616	0	0
UA-2	0	0	0	0	0	0	0	0	0	0	0	0	0	0
UB-1	0	0	0	0	0	0	0	0	0	0	0	0	0	0.675
UB-2	0	0	0	0	0	0	0	0	0	0	0	0	0	0
UB-3	0	0	0	0	0	0	0	0	0	0	0	0	0	0.278
UG-1	0	0	0	0	0	0	0	0	0	0	0	0	0	0
UG-1-2	0	0	0	0	0	0	0	0	0	0	0	0	0	0
UG-2	0	0	0	0	0	0	0	0	0	0	0	0	0	0
UM-1	0	0	0	0	0	0	0	0	0	0	0	0	0	0
UR-1	0	0	0	0	0	0	0	0	0	0	0	0	0	0
V.1-2	0	0	0	0	0	0	0	0	0	0	0	0	0	0.03
VI.2-3	0	0	0	0	0	0	0	0	0	0	0	0	0	0
VI.4	0	0	0	0	0	0	0	0	0	0	0	0	0	0.356
VI.7	0	0	0	0	0	0	0	0	0	0	0	0	0	0
VI.8	0	0	0	0	0	0	0	0	0	0	0	0	0	0
VII.1	0	0	0	0	0	0	0	0	0	0	0	0	0	0
VII.1-3	0	0	0	0	0	0	0	0	0	0	0	0	0	0
VII.3	0	0	0	0	0	0	0	0	0	0	0	0	0	0

Appendix C 4: Adjusted error matrix

ECOCODE	UB-3	UG-1	UG-1-2	UG-2	UM-1	UR-1	V.1-2	VI.2-3	VI.4	VI.7	VI.8	VII.1	VII.1-3	VII.3
H-REST	0	0	0	0	0	0	0	0	0	0	0	0	0	0
HA-1	0	0	0	0.109	0	0	0	0	0	0	0	0	0	0
HA-2	0	0	0	0	0	0	0	0	0	0	0	0	0	0
HB-1	0.055	0	0	0	0	0	0	0	0.055	0	0	0	0	0
HB-2	0	0	0	0	0	0.105	0	0	0.161	0	0	0	0	0
HB-3	0	0	0	0	0	0	0	0	0.161	0	0	0	0	0
HG-1	0	0.101	0	0.172	0	0	0	0	0	0	0	0	0	0
HG-1-2	0	0.118	0	0	0	0	0.129	0	0	0	0	0	0	0
HG-2	0	0.084	0	0.288	0	0.027	0	0	0	0	0	0	0	0
HM-1	0	0	0	0	0	0	1	0	0	0	0	0	0	0
HR-1	0	0.093	0	0	0	0.138	0	0	0	0	0	0	0	0
I.1	0	0	0	0	0	0	0	0	0	0	0	0	0	0
II.2	0	0	0	0	0	0	0	0.142	0	0	0	0	0	0
III.2-3	0	0	0	0	0	0	0	0	0	0	0	0	0	0
IV.8-9	0	0	0	0	0	0	0	0.166	0	0	0	0	0	0
IX.a	0	0	0	0	0	0	0	0	0	0	0	0	0	0
O-U-REST	0	0	0	0	0	0	0	0	0	0	0	0	0	0
O-UA-1	0	0	0	0	0	0	0	0	0	0	0	0	0	0
O-UA-2	0	0	0	0.982	0	0	0	0	0	0	0	0	0	0
O-UB-1	0	0	0	0	0	0	0	0.32	0	0	0	0	0	0
O-UB-2	0	0	0	0.049	0	0.098	0	0	0.049	0	0.049	0	0	0
O-UB-3	0.15	0	0	0	0	0.05	0	0	0	0	0	0	0	0
O-UG-1	0	0.083	0	0	0	0	0	0	0	0	0	0	0	0
O-UG-1-2	0	0	0	0	0	0	0	0	0	0	0	0	0	0
O-UG-2	0	0	0	0	0	0.292	0	0	0	0	0	0	0	0
O-UK-1	0	0	0.05	0	0	0	0	0	0	0	0	0	0	0
O-UR-1	0.126	0	0	0	0	0	0	0.367	0	0	0	0	0	0
OK-1	0	0	0	0	0	0	0	0	0	0	0	0	0	0
R	0	0	0	0	0	0	0	0	0	0	0	0	0	0
REST	0	0	0	0	0	0	0	0	0	0	0	0	0	0
RnM	0	0	0	0	0	0	0	0	0	0	0	0	0	0
RvD	0	0	0	0	0	0	0	0	0	0	0	0	0	0
RvM	0	0	0	0	0	0	0	0	0	0	0	0	0	0
RvO	0	0	0	0	0	0	0	0	0	0	0	0	0	0
RwD	0	0	0	0	0	0	0	0	0	0	0	0	0	0
RwM	0	0	0	0	0	0	0	0	0	0	0	0	0	0
RwO	0	0	0	0	0	0	0	0	0	0	0	0	0	0
RzD	0	0	0	0	0	0	0	0	0	0	0	0	0	0
RzM	0	0	0	0	0	0	0	0	0	0	0	0	0	0
RzO	0	0	0	0	0	0	0	0	0	0	0	0	0	0
U-REST	0	0	0	0	0	0	0	0	0	0	0	0	0	0
UA-1	0	0	0	0.184	0	0	0	0	0	0	0	0	0	0
UA-2	0	0	0	0.243	0	0	0	0	0	0	0	0	0	0
UB-1	0	0	0	0	0	0	0	0.03	0.08	0	0	0	0	0
UB-2	0.105	0	0	0	0	0	0	0.123	0	0	0	0	0	0
UB-3	0.346	0	0	0.139	0	0	0	0	0	0	0	0	0	0
UG-1	0	0.21	0	0.096	0	0.192	0	0	0	0	0	0.096	0	0
UG-1-2	0	0.246	0	0.271	0	0	0	0	0	0	0	0	0	0
UG-2	0	0.322	0	0.325	0	0.085	0	0.042	0	0	0	0.036	0	0
UM-1	0	0	0	0	0	0	0.552	0	0	0	0	0	0	0
UR-1	0	0.035	0	0	0	0.627	0.08	0	0	0.094	0	0	0	0
V.1-2	0	0.08	0	0	0	0.229	0	0.16	0	0	0	0	0	0
VI.2-3	0	0	0	0	0	0.097	0	0.352	0.168	0	0	0	0.071	0
VI.4	0	0	0	0	0	0	0	0.032	0.193	0	0	0	0	0
VI.7	0	0	0	0	0	0	0	0	0	0	0	0	0	0
VI.8	0.212	0	0	0	0	0	0	0	0	0	0	0	0	0
VII.1	0	0.378	0	0	0	0	0	0	0	0	0	0.433	0	0
VII.1-3	0	0	0	0	0	0	0	0	0	0	0	0.496	0.183	0
VII.3	0	0.358	0	0	0	0	0	0	0	0	0	0	0	0